

Lifting the Veil: Unlocking the Power of Depth in Q-learning

Shao-Bo Lin, Tao Li, Shaojie Tang, Yao Wang, Ding-Xuan Zhou

Abstract—With the help of massive data and rich computational resources, deep Q-learning has been widely used in operations research and management science and has contributed to great success in numerous applications, including recommender systems, supply chains, games, and robotic manipulation. However, the success of deep Q-learning lacks solid theoretical verification and interpretability. The aim of this paper is to theoretically verify the power of depth in deep Q-learning. Within the framework of statistical learning theory, we rigorously prove that deep Q-learning outperforms its traditional version by demonstrating its good generalization error bound. Our results reveal that the main reason for the success of deep Q-learning is the excellent performance of deep neural networks (deep nets) in capturing the special properties of rewards namely, spatial sparseness and piecewise constancy, rather than their large capacities. In this paper, we make fundamental contributions to the field of reinforcement learning by answering to the following three questions: Why does deep Q-learning perform so well? When does deep Q-learning perform better than traditional Q-learning? How many samples are required to achieve a specific prediction accuracy for deep Q-learning? Our theoretical assertions are verified by applying deep Q-learning in the well-known beer game in supply chain management and a simulated recommender system.

Index Terms—deep Q-learning, deep nets, reinforcement learning, generalization error, beer game, recommender system.



1 INTRODUCTION

Intelligent system operations [1], supply chain management [2], production recommendation [3], human resource management [4], games [5], robotic manipulation [6], pricing [4], and many other applications, often deal with data consisting of states, actions and rewards. Developing suitable policies based on these data to improve the quality of decision-making is an important research topic in operations research and management science. For example, in product recommendations [3], the state refers to a user's current preference, the action is the recommendation of a product to the user, and the reward concerns his/her feedback on the recommendation. The goal is to find a policy that efficiently recommends products that can maximize the cumulative rewards and thus increase revenue. To address these sequential decision-making problems, traditional studies [7] favour *model-driven* approaches; many models are proposed based on human ingenuity and prior knowledge and data are utilized to select a suitable model from these candidates. Such approaches benefit from theoretical analysis and interpretability [8], [9], which are crucial for convincing the decision-makers and persuading consumers. However, these approaches have weak predictive accuracy and are usually labor intensive, frequently requiring people to change the model, as long as some outliers are discovered.

Shao-Bo Lin, Tao Li and Yao Wang are with the Center for Intelligent Decision-making and Machine Learning, School of Management, Xi'an Jiaotong University, Xi'an, China. (email: sblin1983@gmail.com; litt1024@gmail.com; yao.s.wang@gmail.com).

Shaojie Tang is with the Naveen Jindal School of Management, The University of Texas at Dallas, Richardson, Texas, USA. (email: Shaojie.Tang@utdallas.edu).

Ding-Xuan Zhou is with School of Mathematics and Statistics, University of Sydney, Sydney, Australia. (email: dingxuan.zhou@sydney.edu.au).

(Corresponding author: Yao Wang)

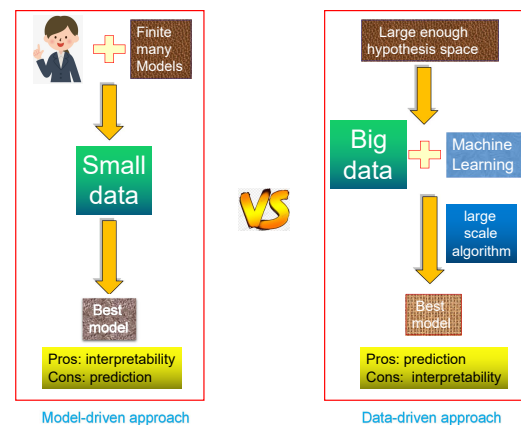


Fig. 1. Philosophy behind *model-driven* and *data-driven* approaches

Meanwhile, the rapid development of data mining in recent years has led to an explosion in the volume and variety of data. These massive data certainly bring opportunities to discover subtle population patterns, but significantly impact labor-intensive model-driven approaches [10]. *Data-driven* approaches, on the other hand, focus on utilizing machine learning methods to explore the patterns suggested by the data. They have attracted growing interest recently in operations research and management science [11], [12], [13], [14]. The basic idea of a data-driven approach is to first adopt a large hypothesis space, with the intuition that the space is rich enough to contain the optimal model, and then apply a specific machine learning algorithm to the massive data to tune a high-quality model from the hypothesis space. These approaches greatly reduce the importance of human ingenuity and improve the prediction accuracy. Figure 1

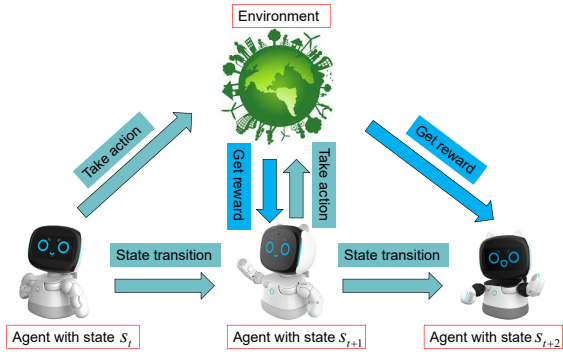


Fig. 2. States, actions and rewards in RL

differentiates the two aforementioned approaches.

However, although the data-driven approach has been widely applied and achieved great success in numerous applications [3], [5], [14], [15], solid theoretical verification and interpretability are needed to support its excellent performance, without which decision makers' enthusiasm may be dampened and they turn to the model-driven approach, neglecting the outstanding performance of the data-driven approach in practice. Under these circumstances, a corresponding theory that explains the running mechanisms and verifies the feasibility of the data-driven approach should be developed urgently, which is the purpose of this paper.

1.1 Problem formulation

Reinforcement learning (RL) [16] is a promising data-driven approach to tackle sequential decision-making problems with data consisting of states, actions, and rewards. As shown in Figure 2, RL aims to develop a sequence of actions to maximize the total cumulative reward. It has been successfully used in human resource operations [17], recommendations [3], games [5], supply chains [2], among others. The review [18] provides additional details on RL.

The Q-learning [19] algorithm is widely used to produce a sequence of high-quality actions in RL and is regarded to be one of the most important breakthroughs in RL [16, Sec. 6.5]. The core of Q-learning is to learn a sequence of Q-functions that are approximations of the optimal values. Q-learning is, by definition, a temporal-difference algorithm that incorporates four components: hypothesis space selection, optimization strategy designation, Q-functions training, and policy search. The hypothesis space component is devoted to selecting a suitable class of functions that regulate some a-priori knowledge of Q-functions. The optimization component entails the mathematical formulation of a series of optimization problems concerning Q-functions based on the given data and selected hypothesis space. The Q-functions component aims to successively determine Q-functions at different times by solving the formulated optimization problems. The policy component determines the policy by maximizing the obtained Q-functions.

As a starting point of Q-learning, the hypothesis space plays a crucial role in Q-learning because it not only regulates the format and property of the Q-function to be learned but also determines the difficulty of solving

the corresponding optimization problems. Since optimal Q-functions are unknown, the selection of hypothesis spaces is an eternal problem in Q-learning [20]. In particular, large hypothesis spaces are beneficial for representing any Q-functions but inevitably require large computations and are frequently unstable to noise. Conversely, excessively small hypothesis spaces lack expressive powers and usually exclude the optimal Q-functions, causing Q-learning to underperform, even in fitting the given data. Due to the limitation of computation and memory requirements, linear spaces spanned by certain basis functions are often selected as hypothesis spaces in traditional Q-learning [16], resulting in several bottlenecks in practice. For example, in robotic grasping [21], Q-learning with linear hypothesis spaces is only applicable to training individual skills, such as hitting a ball, throwing, or opening a door.

With the development of rich computational resources, such as the computational power of modern graphics processing units (GPUs), adopting large hypothesis spaces in Q-learning has become practically feasible. Deep Q-learning, which adopts deep neural networks (or *deep nets*) to build hypothesis spaces, has been used in numerous applications. For instance, AlphaGo [5] beats a professional human "go" player in a complete game of Go without handicap; deep robotic grasping [6] achieved a 96% grasp success rate on unseen objects, and certain bottlenecks in traditional Q-learning have been overcome [21].

Despite its great success in practice, deep Q-learning lacks the theoretical foundations to provide the guarantees required by many applications. Consequently, the ability of deep Q-learning to outperform existing schemes is unclear, and users hesitate to adopt deep Q-learning in safety-critical learning tasks, such as clinical diagnosis and financial investment. The following three crucial questions should be answered to increase the confidence of decision-makers:

- ◇ **Question 1.** Why does deep Q-learning perform so well?
- ◇ **Question 2.** When does deep Q-learning perform better than traditional Q-learning?
- ◇ **Question 3.** How many samples are required to achieve a specific prediction accuracy for deep Q-learning?

1.2 Our Contributions

An intuitive explanation for the success of deep Q-learning is the large capacity of deep nets [12], [15], which improves the expressive power of traditional linear hypothesis spaces. In this paper, we demonstrate that this large capacity is not the determining factor, since such a feature makes the learning scheme sensitive to noise and thus leads to large variances [22]. We rigorously prove that the success of deep nets in Q-learning is due to their excellent performance in capturing the locality, spatial sparseness, and piecewise smoothness of rewards, which is beyond the capability of shallow nets and linear models [23]. In particular, after analyzing the relationship between optimal Q-functions and rewards, we find that optimal Q-functions are generally spatially sparse and piecewise smooth. With similar capacities, deep nets outperform shallow nets and linear models by providing a considerably better approximation error. Our main contributions are as follows.

- *Oracle inequality for Q-learning*: An oracle inequality is a bound on the risk of an estimator that shows that the performance of the estimator is almost as good as it would be if the decision-maker had access to an oracle that knows what the best the model should be. It is an important tool that determines whether the estimator in hand is optimal. Our first contribution is the establishment of an oracle inequality for Q-learning, which shows the crucial role of hypothesis spaces. We adopt two conflicting quantities, namely, approximation error and covering numbers, to illustrate a dilemma in selecting hypothesis spaces. The optimal performance is achieved by balancing these two quantities.

- *Expressivity for deep nets without enlarging the capacity*: Generally speaking, it is difficult to select hypothesis spaces with both small approximation errors and covering numbers. However, in Q-learning, optimal Q-functions depend heavily on rewards, and the adopted rewards are usually spatially sparse and piecewise smooth [16]. Our results rigorously demonstrate the advantage of deep nets in approximating spatially sparse and piecewise-smooth functions. The approximation capability of deep nets is substantially better than that of linear models and shallow nets that have almost the same capacities. This finding addresses Question 1 and shows that the reason why deep Q-learning outperforms traditional Q-learning is due to its innovation of selecting hypothesis spaces that possess both small approximation errors and covering numbers, provided the rewards are spatially sparse and piecewise-smooth functions. With this, we provide a basis for answering Question 2, that is, understanding when deep Q-learning outperforms traditional Q-learning.

- *Generalization error for deep Q-learning*: Combining the approximation error estimate and the established oracle inequality, we succeed in deriving a tight generalization error bound for deep Q-learning and answering Question 3. Since deep nets can capture the spatial sparseness and piecewise smoothness of rewards, the derived generalization error is smaller than that of traditional Q-learning with linear hypothesis spaces, which shows the power of depth in deep Q-learning.

- *Numerical verifications*: Motivated by [14] and [24], we apply deep Q-learning to a classical supply chain management problem: the beer game, and a simulated recommender system. We numerically show that if the reward is incorrectly specified, then deep Q-learning cannot essentially improve the performance of the classical (shallow) Q-learning approach. The effectiveness and efficiency of deepening the network are based on the appropriate reward. A similar conclusion holds for the role of data size in deep Q-learning in terms that massive data can embody the advantage of deep Q-learning, whereas small data cannot do it. These interesting phenomena numerically verify our theoretical assertions that the properties of rewards, depth of neural networks, and size of data are three crucial factors that guarantee the excellent performance of deep Q-learning.

1.3 Organization

The rest of this paper is organized as follows. In Section 3, we explain RL and Q-learning and present a novel oracle

inequality for Q-learning. In Section 4, we introduce several important properties of optimal Q-functions and show the performance of deep nets in approximating these Q-functions. In Section 5, we pursue the power of depth by exhibiting a tight generalization error of deep Q-learning. In Section 6, we conduct experiments by applying deep Q-learning to the beer game and recommender system to verify our theoretical assertions. We draw a simple conclusion in the last section. The proofs of our results and the background of the beer game and recommender system application are presented in the supplementary material.

2 RELATED WORK

Over the past decade, RL has been shown to be a powerful tool for addressing sequential decision-making problems. An important reason for this is its integration with deep nets [25]. Although the power of depth in deep Q-learning remains undetermined, there are numerous studies on the generalization capability of traditional Q-learning, the power of depth in supervised learning, and the feasibility of deep Q-learning, which are related to our work.

Unlike classical works [26], [27], [28] describing the convergence of Q-learning for finite-horizon RL problems, the present paper focuses on the generalization capability, which quantifies the relationship between the prediction accuracy and number of samples. The generalization capability of Q-learning, measured by the generalization error (or finite-sample bounds), has proven a stumbling block for an enormous number of research activities over the past twenty years [29], [30], [31], [32], [33], [34]. Among these works, [29], [31] are the most related to our work, where the generalization error of batch Q-learning is deduced for finite-horizon sequential decision-making problems. The novelty of our work is that we highlight the important role of hypothesis spaces in Q-learning rather than assuming the hypothesis spaces to be linear models. Furthermore, under the same conditions, our derived generalization error bound is much smaller than those of [29], [31], since several new techniques have been developed, such as a novel error decomposition and a new concentration inequality for Q-learning.

The approximation capability of neural networks is a classical research topic that back to the 1980s, when the universal approximation property of shallow nets was established by [35]. A common consensus is that the power of depth depends heavily on the properties of target functions. If the target function is smooth, then it was proved by [36] that deep nets perform similarly to shallow nets, showing that there is no essential improvement when the approximation tools change from shallow nets to deep nets. For complicated functions, deep nets have been shown to be much better than shallow nets and linear models. In particular, with a comparable number of free parameters, Deep nets have been proven to outperform shallow nets and linear models in embodying the manifold structures of the input space [37], realizing the sparseness in the frequency domain [38] and spatial domain [39], reflecting the rotation-invariance of the data [40], grasping the hierarchical features of the data [41], and approximating non-smooth functions [42]. All these demonstrate the power of depth in supervised

learning. In this paper, we aim to derive the advantage of deep nets in approximating optimal Q-functions, which are piecewise smooth and spatially sparse in numerous applications [16]. We rigorously prove that deep nets outperform shallow nets and linear models in approximating such Q-functions and show the reasonableness and efficiency of building hypothesis spaces using deep nets.

To the best of our knowledge, [43] is the first work to show the feasibility of deep Q-learning in terms of generalization. Under some composition and smoothness assumptions for optimal Q-functions and a concentration coefficient assumption regarding marginal probability, [43] derived a generalization error estimate of deep Q-learning and showed that deep Q-learning beats the classical version, which is, of course, a beneficial development that lays a stepping-stone toward understanding deep Q-learning. There are three main differences between our work and that of [43]. The first difference is the setting; we are concerned with finite-stage sequential decision-making problems, whereas [43] considered infinite-stage problems involving strict restrictions on the discount factor to guarantee the concentration coefficient assumption. The second difference is the adopted algorithms, although both are variants of batch Q-learning. To be detailed, since infinite-stage sequential decision-making problems are considered in [43], the policy length was a main parameter and depended heavily on the concentration coefficient assumption, which is difficult to verify in practice; this is not the case in our analysis. The last difference is the assumptions of the optimal Q-functions; our assumptions are induced from numerous deep Q-learning applications, which is beyond the scope of [43].

Another recent paper [14] studied the performance of deep Q-learning in inventory optimization problems. The basic idea was to adopt a shaped variant of rewards, with which they showed that deep Q-learning can essentially improve the performance of classical (shallow) Q-learning. Our numerical studies are motivated by [14]. However, unlike [14], which showed the outperformance of shaped deep Q-learning, we numerically elucidate the roles of depth, rewards and data size. We apply a similar numerical experiment in a simulated recommender system [44]. Our numerical results aim to reveal the veil of the success of deep Q-learning. More importantly, we derive a solid theoretical analysis to show why and when deep Q-learning outperforms classical (shallow) Q-learning. Our theoretical results can provide a theoretical guarantee for [14] and [24].

3 ORACLE INEQUALITY FOR Q-LEARNING

We present an oracle inequality to show the important role of hypothesis spaces in Q-learning. Throughout the paper, we use upper-case letters to denote random variables and lower-case letters to denote instances of random variables.

3.1 RL and Q-learning

We consider T -stage sequential decision-making problems. For $t = 1, \dots, T$, let $\tilde{\mathcal{S}}_t \subset \mathbb{R}^{d_{s,t}}$ and $\tilde{\mathcal{A}}_t \subset \mathbb{R}^{d_{a,t}}$ be families of states and actions, respectively, in stage t , where $d_{s,t}, d_{a,t} \in \mathbb{N}$ denote the dimensions of the state and action spaces at

stage t . The data in RL are formed as $\mathcal{T}_T = (\mathbf{s}_{T+1}, \mathbf{a}_T, \mathbf{R}_T)$, where $\mathbf{s}_t = \{s_1, \dots, s_t\}$ with $s_t \in \tilde{\mathcal{S}}_t$ is the sequence of t states, $\mathbf{a}_t = \{a_1, \dots, a_t\}$ with $a_t \in \tilde{\mathcal{A}}_t$ is the sequence of t actions, and $\mathbf{R}_t = \{R_1, \dots, R_t\}$ with $R_t := R_t(\mathbf{s}_{t+1}, \mathbf{a}_t)$ is the sequence of t rewards. Denote by $D := \{\mathcal{T}_{T,i}\}_{i=1}^m$ the training set of size m . RL aims to derive T maps as

$$\pi_t : \tilde{\mathcal{S}}_1 \times \dots \times \tilde{\mathcal{S}}_t \times \tilde{\mathcal{A}}_1 \times \dots \times \tilde{\mathcal{A}}_{t-1} \rightarrow \tilde{\mathcal{A}}_t, t = 1, 2, \dots, T$$

to maximize $\sum_{t=1}^T R_t(\mathbf{s}_{t+1}, \pi_t(\mathbf{s}_t, \mathbf{a}_{t-1}))$ based on D .

Under the standard statistical framework of RL [20], [29], [31], samples in $\{\mathcal{T}_{T,i}\}_{i=1}^m$ are assumed to be drawn independently and identically (i.i.d.) according to a definite but unknown distribution

$$P = \rho_1(s_1)p_1(a_1|s_1) \prod_{t=2}^T \rho_t(s_t|\mathbf{s}_{t-1}, \mathbf{a}_{t-1})p_t(a_t|\mathbf{s}_t, \mathbf{a}_{t-1})\rho_{T+1}(s_{T+1}|\mathbf{s}_T, \mathbf{a}_T), \quad (1)$$

where $\rho_t(s_t|\mathbf{s}_{t-1}, \mathbf{a}_{t-1})$ is the conditional density of s_t conditioned on $\mathbf{s}_{t-1}, \mathbf{a}_{t-1}$ and $p_t(a_t|\mathbf{s}_t, \mathbf{a}_{t-1})$ denotes the probability that action a_t is taken given the history $\{\mathbf{s}_t, \mathbf{a}_{t-1}\}$. A policy formed by a sequence of decision rules is written as $\pi = \{\pi_1, \dots, \pi_T\}$. We further denote

$$P_\pi = \rho_1(s_1)1_{a_1=\pi_1(s_1)} \prod_{t=2}^T \rho_t(s_t|\mathbf{s}_{t-1}, \mathbf{a}_{t-1})1_{a_t=\pi(\mathbf{s}_t, \mathbf{a}_{t-1})}\rho_{T+1}(s_{T+1}|\mathbf{s}_T, \mathbf{a}_T), \quad (2)$$

where for a predicate W , 1_W is 1 if W is true and 0 otherwise.

Define the t value function (value function at time t) of π by

$$V_{\pi,t}(\mathbf{s}_t, \mathbf{a}_{t-1}) = E_\pi \left[\sum_{j=t}^T R_j(\mathbf{S}_{j+1}, \mathbf{A}_j) | \mathbf{S}_t = \mathbf{s}_t, \mathbf{A}_{t-1} = \mathbf{a}_{t-1} \right],$$

where E_π is the expectation with respect to the distribution P_π . If $t = 1$, then this can be written as $V_\pi(s_1) = V_{\pi,1}(s_1)$ for brevity. We further denote the optimal t value function as

$$V_t^*(\mathbf{s}_t, \mathbf{a}_{t-1}) = \max_{\pi \in \Pi} V_{\pi,t}(\mathbf{s}_t, \mathbf{a}_{t-1}),$$

where Π denotes the collection of all policies. The Bellman equation [45] characterizes the optimal policy π^* as

$$\begin{aligned} \pi_t^*(\mathbf{s}_t, \mathbf{a}_{t-1}) &= \arg \max_{a_t} E[R_t(\mathbf{S}_{t+1}, \mathbf{A}_t) \\ &\quad + V_{t+1}^*(\mathbf{S}_{t+1}, \mathbf{A}_t) | \mathbf{S}_t = \mathbf{s}_t, \mathbf{A}_t = \mathbf{a}_t], \end{aligned} \quad (3)$$

where E is the expectation with respect to P . RL then aims to find a policy $\hat{\pi}$ to minimize $V^*(s_1) - V_{\hat{\pi}}(s_1)$, where $V^*(s_1) := V_1^*(s_1)$.

Batch Q-learning [16], [29], a widely used variant of Q-learning, divides a T -stage sequential decision-making problem into T least squares problems. The optimal time-dependent Q-function is defined by

$$\begin{aligned} Q_t^*(\mathbf{s}_t, \mathbf{a}_t) &= E[R_t(\mathbf{S}_{t+1}, \mathbf{A}_t) \\ &\quad + V_{t+1}^*(\mathbf{S}_{t+1}, \mathbf{A}_t) | \mathbf{S}_t = \mathbf{s}_t, \mathbf{A}_t = \mathbf{a}_t]. \end{aligned} \quad (4)$$

Since

$$\begin{aligned} & V_t^*(\mathbf{s}_t, \mathbf{a}_{t-1}) \\ &= V_{\pi^*, t}(\mathbf{s}_t, \mathbf{a}_{t-1}) \\ &= E_{\pi^*} \left[\sum_{j=t}^T R_j(\mathbf{S}_{j+1}, \mathbf{A}_j) \mid \mathbf{S}_t = \mathbf{s}_t, \mathbf{A}_{t-1} = \mathbf{a}_{t-1} \right], \end{aligned}$$

then

$$V_t^*(\mathbf{s}_t, \mathbf{a}_{t-1}) = \max_{a_t} Q_t^*(\mathbf{s}_t, \mathbf{a}_t). \quad (5)$$

We call $V_t^*(\mathbf{s}_t, \mathbf{a}_{t-1}) - Q_t^*(\mathbf{s}_t, \mathbf{a}_t)$ the optimal advantage temporal-difference at time t . Furthermore, according to [29, Lemma 1] (see also [46, Chap. 5]),

$$\begin{aligned} & V^*(s_1) - V_{\pi}(s_1) = \\ & E_{\pi} \left[\sum_{t=1}^T V_t^*(\mathbf{S}_t, \mathbf{A}_{t-1}) - Q_t^*(\mathbf{S}_t, \mathbf{A}_t) \mid S_1 = s_1 \right] \quad (6) \end{aligned}$$

holds for an arbitrary π . This equality shows that the quality of a policy π depends on the temporal difference, and a good estimate of optimal Q-function helps reduce the generalization error of RL. Under these circumstances, the estimation of Q_t^* for $t = 1, \dots, T$ lies at the core of batch Q-learning. With $Q_{T+1}^* = 0$, it follows from (4) and (5) that for $t = T, T-1, \dots, 1$,

$$\begin{aligned} Q_t^*(\mathbf{s}_t, \mathbf{a}_t) &= E[R_t(\mathbf{S}_{t+1}, \mathbf{A}_t) \\ &+ \max_{a_{t+1}} Q_{t+1}^*(\mathbf{S}_{t+1}, \mathbf{A}_t, a_{t+1}) \mid \mathbf{S}_t = \mathbf{s}_t, \mathbf{A}_t = \mathbf{a}_t] \quad (7) \end{aligned}$$

This implies the following proposition.

Proposition 1: Let L_t^2 be the space of square-integrable functions with respect to the distribution

$$P_t = \rho_1(s_1) p_1(a_1 \mid s_1) \prod_{j=2}^t \rho_j(s_j \mid \mathbf{s}_{j-1}, \mathbf{a}_{j-1}) p_j(a_j \mid \mathbf{s}_j, \mathbf{a}_{j-1}). \quad (8)$$

Then, for $t = T, T-1, \dots, 1$, we have

$$\begin{aligned} Q_t^*(\mathbf{s}_t, \mathbf{a}_t) &= \arg \min_{Q_t \in L_t^2} E[(R_t(\mathbf{S}_{t+1}, \mathbf{A}_t) \\ &+ \max_{a_{t+1}} Q_{t+1}^*(\mathbf{S}_{t+1}, \mathbf{A}_t, a_{t+1}) - Q_t(\mathbf{S}_t, \mathbf{A}_t))^2]. \quad (9) \end{aligned}$$

According to Proposition 1, optimal Q-functions can be obtained by solving T least squares problems via the backward recursion, that is, $t = T, T-1, \dots, 1$. Empirically, by setting $\hat{Q}_{T+1} = 0$, we can compute Q-functions (\hat{Q}_t for $t = T, T-1, \dots, 1$) by solving the following T least squares problems

$$\begin{aligned} \hat{Q}_t(\mathbf{s}_t, \mathbf{a}_t) &= \arg \min_{Q_t \in \tilde{\mathcal{Q}}_t} \mathbb{E}_m[(R_t(\mathbf{S}_{t+1}, \mathbf{A}_t) \\ &+ \max_{a_{t+1}} \hat{Q}_{t+1}(\mathbf{S}_{t+1}, \mathbf{A}_t, a_{t+1}) - Q_t(\mathbf{S}_t, \mathbf{A}_t))^2], \quad (10) \end{aligned}$$

where \mathbb{E}_m is the empirical expectation and $\tilde{\mathcal{Q}}_t$ is a parameterized hypothesis space. With this, we obtain a sequence of estimators $\{\hat{Q}_T, \dots, \hat{Q}_1\}$ and define the corresponding policy by

$$\hat{\pi}_t(\mathbf{s}_t, \mathbf{a}_{t-1}) = \arg \max_{a_t \in \tilde{\mathcal{A}}_t} \hat{Q}_t(\mathbf{s}_t, \mathbf{a}_{t-1}, a_t), t = 1, \dots, T. \quad (11)$$

3.2 Oracle inequality for Q-learning

In this subsection, we aim to derive our novel oracle inequality for Q-learning. We first introduce two mild assumptions.

Assumption 1: Let $\mu \geq 1$ be a constant. Then,

$$p_t(a \mid \mathbf{s}_t, \mathbf{a}_{t-1}) \geq \mu^{-1}, \quad \forall a \in \tilde{\mathcal{A}}_t. \quad (12)$$

Assumption 1 is a standard assumption made in [29, [31] and it states that every action in $\tilde{\mathcal{A}}_t$ has a positive conditional probability of being chosen at each time t . It contains at least two widely used settings. One is that $\tilde{\mathcal{A}}_t$ only contains finitely many actions, which is the case in go games [5], blackjack [16], robotic grasping [6] and beer game [14]. The other is that $\tilde{\mathcal{A}}_t$ is an infinite set, but only finite actions in $\tilde{\mathcal{A}}_t$ are active when in the case of $\{\mathbf{s}_t, \mathbf{a}_{t-1}\}$. For example, in a recommender system, if the feedback for a client's age is around three, then the following candidate action is to recommend children's products. Hence, Assumption 1 is a mild condition that can be easily satisfied for numerous applications. Since rewards are given before the learning process and are always assumed to be finite, we present the following mild assumption.

Assumption 2: There exists a $U > 0$ such that $\|R_t\|_{L^\infty} \leq U$ for any $t = 1, \dots, T$.

According to (7) and $Q_{T+1}^* = 0$, Assumption 2 implies that $\|Q_t^*\|_{L^\infty} \leq 2U$ for all $t = 1, 2, \dots, T$. Therefore, it is natural to search for estimators uniformly bounded by $2U$. To describe the role of hypothesis space, we also introduce the empirical covering number [9], [47] to quantify its capacity. For a set of functions \mathcal{G} defined on $\mathcal{X} \subseteq \mathbb{R}^d$ with $d \in \mathbb{N}$, denote by $\mathcal{N}_1(\epsilon, \mathcal{G}, x_1^m)$ with $x_1^m = (x_1, \dots, x_m) \in \mathcal{X}^m$ the ℓ^1 empirical covering number [47, Def.9.3] of \mathcal{G} , which is the number of elements in a least ϵ -net of \mathcal{G} with respect to $\|\cdot\|_{\ell^1}$. Furthermore, let $\mathcal{N}_1(\epsilon, \mathcal{G}) := \max_{x_1^m \in \mathcal{X}^m} \mathcal{N}_1(\epsilon, \mathcal{G}, x_1^m)$. We then obtain the following oracle inequality for batch Q-learning.

Theorem 1: Let $\beta_t > 0$, $\tilde{\mathcal{Q}}_t, t = 1, \dots, T$ be sets of functions uniformly bounded by $2U$ and $\tilde{\mathcal{Q}}_{T+1} = \{0\}$. If Assumptions 1 and 2 hold and \hat{Q}_t is defined by (10), then

$$\begin{aligned} & E[V^*(S_1) - V_{\pi}(S_1)] \leq \\ & C \sum_{t=1}^T \sum_{j=t}^T (3\mu)^{j-t} \left(\min_{h_j \in \tilde{\mathcal{Q}}_j} E[(h_j - Q_j^*)^2] + \beta_j + \frac{1}{m} \right. \\ & \left. + \frac{1}{m} \exp(-C'\beta_j m) (\mathcal{N}_1(C'\beta_j, \tilde{\mathcal{Q}}_j) + \mathcal{N}_1(C'\beta_j, \tilde{\mathcal{Q}}_{j+1})) \right)^{\frac{1}{2}}, \quad (13) \end{aligned}$$

where C and C' are constants depending only on U .

Theorem 1 presents a bias-variance trade-off in selecting the hypothesis space $\tilde{\mathcal{Q}}_t$. If $\tilde{\mathcal{Q}}_t$ is large, then the approximation error $\min_{h_j \in \tilde{\mathcal{Q}}_j} E[(h_j - Q_j^*)^2]$ is small but the capacity $\mathcal{N}_1(C'\beta_j, \tilde{\mathcal{Q}}_j)$ will be large, leading to bad generalization. Conversely, if $\tilde{\mathcal{Q}}_t$ is small, then $\mathcal{N}_1(C'\beta_j, \tilde{\mathcal{Q}}_j)$ is small but its approximation performance is not so good, which will also result in bad generalization. A suitable hypothesis space should be selected to balance the bias and variance in each stage, thereby achieving the best learning performance. The

bias-variance balance is determined by the a-priori information of Q_t^* , without which it is impossible to derive a satisfactory generalization error [47, Chap. 3].

Estimation of the capacity of a hypothesis space is a classical topic in statistical learning theory [22], [47], [48]. In particular, it is discussed in [47, Chap. 9] for linear models of dimension k , \mathcal{G}_k° , and [47, Chap. 16] for shallow nets G_k^* with k tunable parameters and some specified activation function for which

$$\log \mathcal{N}_1(\varepsilon, \mathcal{G}_{k,M}) \leq C_1 k \log \frac{M}{\varepsilon}, \quad \forall \varepsilon > 0, \quad (14)$$

where $\mathcal{G}_{k,M} = \{f \in \mathcal{G}_K, \|f\|_\infty \leq M\}$, \mathcal{G}_k is either \mathcal{G}_k^* or \mathcal{G}_k° , $M > 0$ and C_1 is a constant depending only on M . The following corollary then follows from Theorem 1 with $\beta_t = \frac{2C_1 \max\{k_t, k_{t+1}\} \log(2C'Um)}{C'm}$.

Corollary 1: Let $k_t \in \mathbb{N}$, $k_{T+1} = 0$, $\tilde{Q}_{T+1} = \{0\}$ and \tilde{Q}_t , $t = 1, \dots, T$ be sets of functions satisfying (14) with $k = k_t$ and $M = 2U$. If Assumptions 1 and 2 hold and \hat{Q}_t is defined by (10), then

$$E[V^*(S_1) - V_\pi(S_1)] \leq C'' \sum_{t=1}^T \sum_{j=t}^T (3\mu)^{j-t} \left(\min_{h_j \in \tilde{Q}_j} E[(h_t - Q_t^*)^2] + \frac{\max\{k_t, k_{t+1}\} \log(2m)}{m} \right)^{\frac{1}{2}},$$

where C'' is a constant depending only on U .

The oracle inequality for batch Q-learning was initially deduced by [29] under the same setting as ours. However, there are three crucial differences between our results and those of [29, Theorem 1]. First, we do not assume that $Q_t^* \in \tilde{Q}_t$ and utilize the approximation error to measure the expressive power of \tilde{Q}_t . Since optimal Q-functions are rarely known in practice, the assumption of $Q_t^* \in \tilde{Q}_t$ requires an extremely large hypothesis space, which leads to a large generalization error. Then, the derived generalization error bound in Theorem 1 or Corollary 1 is essentially better than that of [29, Theorem 1] under the same conditions. In particular, if \tilde{Q}_t is a linear space and $Q_t^* \in \tilde{Q}_t$, our derived generalization error in Corollary 1, is of order $\mathcal{O}(m^{-1/2})$, whereas that in [29, Theorem 1] is of order $\mathcal{O}(m^{-1/4})$. Finally, we take the covering number to measure the generalization error without presenting any restrictions on it, which is totally different from [29, Theorem 1] that conducted the analysis under capacity restrictions like (14). This makes our analysis applicable to numerous hypothesis spaces, such as reproducing kernel Hilbert space [49], shallow nets [47, Chap.16] and deep nets [36].

4 DEEP NETS IN APPROXIMATING OPTIMAL Q-FUNCTIONS

In this section, we first demonstrate some good properties of optimal Q-functions of many real-world applications and then analyze the power of depth in approximating Q-functions via deep nets.

4.1 A priori information for optimal Q-functions

We provide some excellent applications of deep Q-learning and present the a-priori information for optimal Q-functions. Q-learning has been proven to gain considerably profitable (long-term) rewards [50] in a recommender system, where the state is defined as the browsing history of a user, and the action is to recommend (one or more item) items to the user and the reward is the user's feedback, including skipping, clicking, or ordering of these items. This implies that the reward function is piecewise constant and spatially sparse with respect to the state and action. Traditional Q-learning adopts linear models to formulate the hypothesis space, which cannot capture piecewise constancy or spatial sparseness [39]. This makes it difficult to design an efficient policy to recommend multiple products simultaneously [3]. Deep Q-learning succeeds in overcoming this bottleneck of traditional Q-learning [3] by recommending numerous high-quality products simultaneously.

Q-learning also provides a promising avenue for manipulating robotic interaction. Traditional Q-learning is only applicable to individual skills, such as hitting a ball, throwing, or opening a door [21]. Consequently, [6] developed a deep Q-learning approach to robotic grasping that achieved a 96% grasp success rate on unseen objects. In their approach, the state includes the robot's current camera observation, and an RGB image with a certain resolution (e.g., 472×472). The action consists of a vector indicating the desired change in the gripper position, such as the open and close commands. The reward is 1 at the end of the episode if the gripper contains an object and is above a certain height, and 0 otherwise, showing the piecewise constant and spatially sparse property of the reward functions.

Q-learning has numerous other applications, where the reward functions are set to be piecewise smooth (or piecewise constant) and spatially sparse. We refer the readers to a detailed beer game example in Section 4 of the supplementary material or some interesting examples in [16] shown in Table 4.1. All these shows that piecewise smoothness (or piecewise constant) and spatial sparseness are two vital properties of reward functions. Under this circumstance, it follows from (7) and $Q_{T+1}^* = 0$ that optimal Q-functions are also piecewise smooth (or piecewise constant) and spatially sparse, as shown in Table 4.1.

In the following, we provide the mathematical definition of spatially sparse and piecewise smooth (or piecewise constant) functions. For $d, N \in \mathbb{N}$ and $\mathbb{I}^d := [0, 1]^d$, we partition \mathbb{I}^d by N^d sub-cubes $\{A_j\}_{j=1}^{N^d}$ of side length N^{-1} and with centers $\{\zeta_j\}_{j=1}^{N^d}$. For $s \in \mathbb{N}$ with $s \leq N^d$ and a function f defined on \mathbb{I}^d , if the support of f is contained in $\cup_{j \in \Lambda_s} A_j$ for some subset Λ_s of $\{1, \dots, N^d\}$ of cardinality s , we then say that f is s spatially sparse in N^d cubic partitions.

Let $c_0 > 0$, $r = u + v$ with $u \in \mathbb{N}_0 := \{0\} \cup \mathbb{N}$, $0 < v \leq 1$, and $\mathbb{A} \subseteq \mathbb{I}^d$. We say that a function $f : \mathbb{A} \rightarrow \mathbb{R}$ is (r, c_0) -smooth, if f is u -times differentiable and for any $\alpha = (\alpha_1, \dots, \alpha_d) \in \mathbb{N}_0^d$ with $\alpha_1 + \dots + \alpha_d = u$ and $x, x' \in \mathbb{A}$, its partial derivative satisfies the Lipschitz condition

$$\left| \frac{\partial^u f}{\partial x_1^{\alpha_1} \dots \partial x_d^{\alpha_d}}(x) - \frac{\partial^u f}{\partial x_1^{\alpha_1} \dots \partial x_d^{\alpha_d}}(x') \right| \leq c_0 \|x - x'\|^v, \quad (15)$$

TABLE 1
Propositions for rewards and optimal Q -functions for games [16]

Games	Rewards	Q^*	References
Pick-and-Place Robot	Piecewise constant	Piecewise constant	Example 3.2
Recycling Robot	Piecewise constant	Piecewise constant	Example 3.3
Pole-Balancing	Piecewise constant	Piecewise constant	Example 3.4
Gridworld	Piecewise constant	Piecewise constant	Example 3.5
Golf	Piecewise constant	Piecewise constant	Example 3.6
Gambler Problem	Piecewise constant	Piecewise constant	Example 4.3
Blackjack	Piecewise constant	Piecewise constant	Example 5.1
Driving Home	Piecewise smooth	Piecewise smooth	Example 6.1
Cliff Walking	Piecewise constant	Piecewise constant	Example 6.6
Dyna Maze	Piecewise constant	Piecewise constant	Example 8.1
Racetrack	Piecewise constant	Piecewise constant	Example 8.6
Mountain Car	Piecewise constant	Piecewise constant	Example 10.1
Access-control Queuing	Piecewise constant	Piecewise constant	Example 10.2
AlphaGo	Piecewise constant	Piecewise constant	Sec. 16.6.1

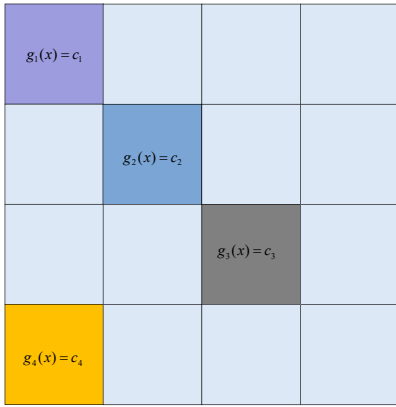


Fig. 3. Piecewise-constant and spatially sparse functions in $\mathcal{C}^{(C_0, 4, 16)}$

where $\|x\|$ denotes the Euclidean norm of x . $Lip_{\mathbb{A}}^{(r, c_0)}$ is then written as the set of functions satisfying (15). If there exists $g_j \in Lip_{A_j}^{(r, c_0)}$ for $j = 1, \dots, N^d$ such that

$$f(x) = \sum_{j \in \Lambda_s} g_j(x) \mathcal{I}_{A_j}(x), \quad (16)$$

we then say that f is s spatially sparse in N^d cubic partitions and (r, c_0) -smooth, where \mathcal{I}_{A_j} is the indicator function of A_j , i.e., $\mathcal{I}_{A_j}(x) = 1$ if $x \in A_j$ and $\mathcal{I}_{A_j}(x) = 0$ if $x \notin A_j$. Denote by $Lip^{(r, c_0, s, N^d)}$ the set of all such functions. A special case of $f \in Lip^{(r, c_0, s, N^d)}$ is $g_j(x) = c_j$ for some $|c_j| \leq C_0$ and $C_0 > 0$. In this case, we say that f is s spatially sparse in N^d cubic partitions and piecewise constant. We further denote by $\mathcal{C}^{(C_0, s, N^d)}$ the set of all these functions. Figure 3 shows a piecewise constant and spatially sparse function in $\mathcal{C}^{(C_0, 4, 16)}$.

4.2 Capacity of deep nets

Let $L \in \mathbb{N}$ and $d_0, d_1, \dots, d_L \in \mathbb{N}$ with $d_0 = d$. For $\vec{h}_k = (h^{(1)}, \dots, h^{(d_k)})^T \in \mathbb{R}^{d_k}$, define $\vec{\sigma}(\vec{h}) = (\sigma(h^{(1)}), \dots, \sigma(h^{(d_k)}))^T$, where $\sigma(t) = \max\{t, 0\}$ is the rectified linear unit (ReLU). Deep nets with depth L and

width d_j in the j th hidden layer can be mathematically represented as

$$h_{\{d_0, \dots, d_L\}}(x) = \vec{a} \cdot \vec{h}_L(x), \quad (17)$$

where

$$\vec{h}_k(x) = \vec{\sigma}(W_k \cdot \vec{h}_{k-1}(x) + \vec{b}^{(k)}), \quad k = 1, 2, \dots, L, \quad (18)$$

$\vec{a} \in \mathbb{R}^{d_L}$, $\vec{b}^{(k)} \in \mathbb{R}^{d_k}$, $\vec{h}_0(x) = x$, and $W_k = (w_{i,j}^{(k)})_{1,1}^{d_k, d_{k-1}}$ is a $d_k \times d_{k-1}$ matrix. The structure of deep nets is reflected by the parameter matrices $(W_k, \vec{b}^{(k)})$. A typical deep net is a deep fully connected neural network (DFCN), which corresponds to weight matrices without any constraints.

We denote by $\mathcal{H}_{\{d_0, \dots, d_L\}}$ the set of all deep nets formed as (17). Then, there are totally

$$n_L := \sum_{j=0}^{L-1} (d_j d_{j+1} + d_{j+1}) + d_L \quad (19)$$

tunable parameters for $h \in \mathcal{H}_{\{d_0, \dots, d_L\}}$. If L is large, there are too many parameters to be tuned, leading to extremely large capacity. It is known that deep sparsely connected nets (DSCN), such as deep convolution neural networks [51], [52], deep nets with tree structures [40] or other sparse structures [42], can significantly reduce the capacity of DFCN without sacrificing its approximation capability very much. The hypothesis spaces in this paper are DSCNs with $n \ll n_L$ tunable parameters paved on L hidden layers. Denote by $\mathcal{H}_{n,L}$ the set of all these deep nets with a specific structure. Thus, we define

$$\mathcal{H}_{n,L,M} := \{h \in \mathcal{H}_{n,L} : \|h\|_{L^\infty} \leq M\}. \quad (20)$$

The following lemma presents a covering number estimate for $\mathcal{H}_{n,L,M}$.

Lemma 1: There is a constant C_1^* depending only on d such that

$$\log \mathcal{N}_1(\epsilon, \mathcal{H}_{n,L,M}) \leq C_1^* L n \log D_{\max} \log \frac{M}{\epsilon}, \quad (21)$$

where $D_{\max} := \max_{0 \leq j \leq L} d_j$.

Since $\|Q_t^*\|_{L^\infty} \leq 2U$, it is natural to take $\mathcal{H}_{n,L,2U}$ as the hypothesis space. It should be mentioned that except for the boundedness of the neural networks, Lemma 1 does not

impose any additional restrictions on the boundedness of weights, which is different from [36] and [53, Chap. 14]. If L is not excessively large, then it follows from (21) and (14) that the covering number of deep nets is comparable with that of shallow nets with n parameters and linear models of n -dimension.

4.3 Approximation capability of deep nets

A common consensus on deep nets' approximation [23], [36], [37], [53], [54], [55], [56] is that the power of depth depends on the properties of target functions. If the target function is assumed to be in $Lip_{\mathbb{R}^d}^{(r, c_0)}$, then [36] verified that deep nets perform similarly to shallow nets, showing that there are no essential improvements when the approximation tools changed from shallow nets or linear models to deep nets. However, if some additional a-priori knowledge is given, deep nets are much more effective than shallow nets and linear models, as Table 2 shows.

TABLE 2
Power of depth in approximating special target functions
(within accuracy ε)

Reference.	Features of target functions	Parameters	Depth
[57]	Locality	$4d + 1$	2
[57]	k -spatially sparse	$k(4d + 1)$	2
[42]	Piecewise (r, c_0) -smooth	$\varepsilon^{-d/r}$	$\mathcal{O}(d, r)$
[58]	ℓ_2 radial + (r, c_0) -smooth	$\varepsilon^{-1/r}$	$\mathcal{O}(d, r)$
[38]	k -sparse (frequency)	$k \log(\varepsilon^{-1})$	$\log(\varepsilon^{-1})$
[37]	d' dimensional manifold+smooth	$\varepsilon^{-d'/r}$	4

As discussed in Sec. 3.1, optimal Q-functions are frequently piecewise constant (or piecewise smooth) and spatially sparse. Studying the advantage of deep nets in approximating such functions is our main purpose, as addressed in the following theorem.

Theorem 2: Let $d \geq 2$, $N \in \mathbb{N}$, $C_0 > 0$, $s \leq N^d$, $1 \leq p < \infty$ and $0 < \tau < 0$. There exists a deep net structure with $L = 2$, $\mathcal{O}(N^d)$ free parameters and $D_{\max} = \mathcal{O}(N^d)$ such that for any $Q^* \in \mathcal{C}^{(C_0, s, N^d)}$, there exists a deep net $\mathcal{N}_{N, s, \tau, Q^*}$ with the aforementioned structure satisfying

$$\|Q^* - \mathcal{N}_{N, s, \tau, Q^*}\|_p \leq 2dC_0s\tau N^{1-d}, \quad (22)$$

where $\|\cdot\|_p$ is the norm of p -times Lebesgue integrable function space $L^p(\mathbb{I}^d)$.

The detailed structure of deep nets in Theorem 2 is given in the proof. Since functions in $\mathcal{C}^{(C_0, s, N^d)}$ are discontinuous in general, linear models [59] suffer from the Gibbs phenomenon in the sense that the linear estimators overshoot at a jump discontinuity, and this overshoot persists as the dimension increases. Shallow nets were utilized in [60] to avoid the Gibbs phenomenon when $d = 1$. For $d \geq 2$, it can be found in [23], [42] that shallow nets are not the optimal approximation tools in the sense that they cannot achieve the optimal approximation rates. In Theorem 2, we rigorously prove that deep nets succeed in overcoming certain drawbacks of linear models and shallow nets in terms of providing perfect approximation error. In fact, we can set τ to be extremely small such that $\|Q^* - \mathcal{N}_{N, s, \tau, Q^*}\|_p \leq \nu$ for arbitrarily small $\nu > 0$. In a word, by adding only

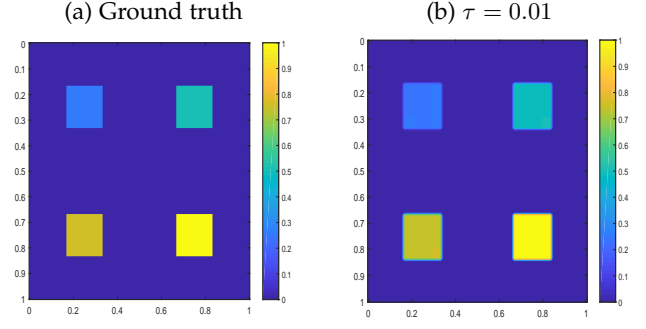


Fig. 4. Performance of deep nets constructed in Theorem 2 with $\tau = 0.01$

one hidden layer to shallow nets, we can use $\mathcal{O}(N^d)$ free parameters to yield an approximant within an arbitrary accuracy, provided the target function is in $\mathcal{C}^{(C_0, s, N^d)}$. As stated in Lemma 1, the ε -covering number of deep nets is of the order $\mathcal{O}(N^d \log \frac{1}{\varepsilon})$, which is the same as that of shallow nets with N^d free parameters and linear models with N^d -dimension. In Figure 4, we provide a numerical example to show the performance of deep nets in approximating functions in $\mathcal{C}^{(1, 4, 36)}$ with $\tau = 0.01$.

In the following theorem, we pursue the power of depth in approximating piecewise smooth and spatially sparse functions.

Theorem 3: Let $1 \leq p < \infty$, $C_0 > 0$, $N, d, s \in \mathbb{N}$, and $r = u + v$ with $u \in \mathbb{N}$ and $0 < v \leq 1$. There exists a deep net structure with

$$2(d + u) \left\lceil \frac{r + 2d}{2d} \right\rceil + 8(d + u) + 3 + \left\lceil \frac{rp + d + p + 1}{2d} \right\rceil \quad (23)$$

layers, nN^d free parameters and $D_{\max} = \text{poly}(N^d n)$ such that for any $Q^* \in Lip^{(r, c_0, s, N^d)}$, there is a $\mathcal{N}_{n, s, N, Q^*}$ with the aforementioned structure satisfying

$$\|Q^* - \mathcal{N}_{n, s, N, Q^*}\|_p \leq C_2^* n^{-r/d} s N^{-d/p},$$

where C_2^* is a constant independent of n, s, N and $\text{poly}(n)$ is a polynomial with respect to n .

Shallow nets were verified in [54] to be at least as good as linear models in the sense that the approximation error of shallow nets is always not larger than that of linear models. The problem is, as mentioned in [40], that the capacity of shallow nets in [54] is usually much larger than that of linear models. This leads to the insatiability of the estimator and a large variance. Furthermore, as discussed above, both linear models and shallow nets are difficult to approximate discontinuous functions. Theorem 3 with $s = N^d$ presents an approximation rate of deep nets when the target function is piecewise smooth, a special type of discontinuous function. It is shown that deep nets can achieve an order of $\mathcal{O}(n^{-r/d})$ when $p = 1$, which is an optimal approximation rate [42] if there are N^d pieces and $N^d n$ parameters.

Besides their discontinuity, optimal Q-functions are spatially sparse, which was not considered in [42]. Theorem 3 is devoted to approximating discontinuous and spatially sparse functions and demonstrates that deep nets outperform shallow nets by showing an additional reducing factor $sN^{-d/p}$ to reflect the sparsity in the approximation error

estimate. It should be highlighted that our result is essentially different from [57], in which the target function is continuous.

In the proofs of Theorems 2 and 3, we shall provide concrete structures of deep nets to approximate spatially sparse and piecewise smooth (or piecewise constant) functions. It should be mentioned that the structure is not unique. In fact, we can derive numerous depth-width pairs of deep nets to achieve the same approximation performance by using the approach in [58]. Furthermore, all these structures can be realized by deep convolutional neural networks via using the technique in [51], [52]. However, since the purpose of our study is to demonstrate the power of depth, we consider only one structure for brevity.

5 POWER OF DEPTH IN DEEP Q-LEARNING

The aim of this section is to show the power of depth in deep Q-learning.

5.1 Learning schemes and assumptions

The main difference between deep Q-learning and the traditional version is their hypothesis spaces. The latter uses linear models, which benefits in computation, whereas the former adopts deep nets to enhance prediction performance. To simplify our analysis, we present a Markov assumption for the distribution P defined by (1).

Assumption 3: Let Q_t^* be defined by (4). We have

$$Q_t^*(\mathbf{s}_t, \mathbf{a}_t) = Q_t^*(s_t, a_t).$$

It should be mentioned that Assumption 3 is not necessary in our analysis, since our result, as shown in Theorem 1, holds for an arbitrary P . Without the Markov assumption, optimal Q-functions (Q_t^* , $t = 1, \dots, T$), are functions with \tilde{d}_t variables with $\tilde{d}_t := \sum_{j=1}^t (d_{a,j} + d_{s,j})$. The fact that $\tilde{d}_{t_1} \leq \tilde{d}_{t_2}$ for $t_1 \leq t_2$ then implies that the hypothesis spaces of deep Q-learning vary with t . Under Assumption 3, if $d_{a,t}$ and $d_{s,t}$ do not vary with t , then Q_t^* , $t = 1, \dots, T$ are functions with the same number of variables, which leads to the same hypothesis space for all times. We also present a compactness assumption for the action and state spaces.

Assumption 4: Assume $\tilde{\mathcal{A}}_t = [0, 1]^{d_{a,t}}$ and $\tilde{\mathcal{S}}_t = [0, 1]^{d_{s,t}}$.

Assumption 4 can be satisfied by using a standard scaling technique directly, provided that the action spaces and state spaces are compact. This is a mild assumption since data are always collected to be bounded. Recall that L_t^2 is the space of square-integrable functions with respect to P_t , as defined in (8). The following distortion assumption describes the difference between P_t and the Lebesgue measure.

Assumption 5: For $p \geq 1$, denote $J_{p,t}$ as the identity mapping: $L_t^2 \xrightarrow{J_p} L^p([0, 1]^{\tilde{d}_t})$ and $\mathcal{J}_{p,T} = \max_{t=1, \dots, T} \|J_{p,t}\|$, where $\|J\|$ is the spectral norm of the operator J . We assume $\mathcal{J}_{p,T} < \infty$.

It is obvious that $\mathcal{J}_{p,t}$ measures the extent to which P_t distorts the Lebesgue measure. Since Q_t^* is frequently spatially sparse, if the support of P_t is out of the support of Q_t^* , then all samples are useless in the learning process,

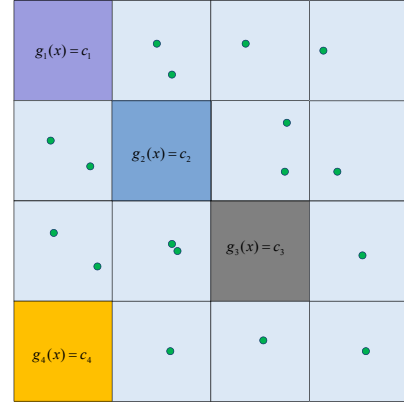


Fig. 5. Support of P_t and sparseness of Q_t^*

as shown in Figure 5. Therefore, Assumption 5 is necessary and reasonable. It holds for all $p \geq 2$ when P_t is the uniform distribution. Then, we present the assumption of spatially sparse and piecewise constant on optimal Q-functions as follows.

Assumption 6: For any $t = 1, \dots, T$, there exist $s_t, N_t \in \mathbb{N}$ such that $Q_t^* \in \mathcal{C}^{(2U, s_t, N_t^{\tilde{d}_t})}$.

As discussed in Sec. 3.1, Assumption 6 is standard for numerous applications. As shown in Theorem 2, each Q_t^* corresponds to a deep net with two hidden layers and $\mathcal{O}(N_t^{\tilde{d}_t})$ free parameters. Denote by $\mathcal{H}_{N_t, \tau, t}$ the set of deep nets structured as in Theorem 2 for $t = 1, \dots, T$. Given the dataset $D = \{\mathcal{T}_{T,i}\}_{i=1}^m = \{(\mathbf{s}_{T+1,i}, \mathbf{a}_{T,i}, \mathbf{R}_{T,i})\}_{i=1}^m$, we can deduce Q-functions via $\hat{Q}_{T+1, N_{T+1}} = 0$ and

$$\hat{Q}_{t, N_t, \tau}(\mathbf{s}_t, \mathbf{a}_t) = \arg \min_{Q_t \in \mathcal{H}_{N_t, \tau, t}} \mathbb{E}_m \left[\left(R_t + \max_{a_{t+1}} \hat{Q}_{t+1}(\mathbf{S}_{t+1}, \mathbf{A}_t, a_{t+1}) - Q_t(\mathbf{S}_t, \mathbf{A}_t) \right)^2 \right].$$

Then, the policy derived from deep Q-learning is defined by

$$\hat{\pi}_{N, \tau} = \{\hat{\pi}_{1, N_1, \tau}, \dots, \hat{\pi}_{T, N_T, \tau}\}, \quad (24)$$

where

$$\hat{\pi}_{t, N_t, \tau}(\mathbf{s}_t, \mathbf{a}_{t-1}) = \arg \max_{a_t \in \tilde{\mathcal{A}}_t} \hat{Q}_{t, N_t}(\mathbf{s}_t, \mathbf{a}_{t-1}, a_t), \quad t = 1, \dots, T. \quad (25)$$

Since N_t and \tilde{d}_t vary with t , the network structures at different times are vary. Further noting that $L = 2$ for all t , we can parameterize the width in the learning process. The following assumption on piecewise smooth and spatially sparse is our final assumption.

Assumption 7: For any $t = 1, \dots, T$, there exist $r_t > 0$, $c_0 > 0$, $s_t, N_t \in \mathbb{N}$ such that $Q_t^* \in Lip^{(r_t, c_0, s_t, N_t^{\tilde{d}_t})}$.

The non-differentiability of ReLU results in the necessity of depth in approximating functions in $Lip_{\mathbb{R}^d}^{(r, c_0)}$. Let $\mathcal{H}_{t, n_t, N_t, L_t}$ be the set of deep nets structured as in Theorem 3 with respect to Q_t^* . We build the hypothesis spaces for Q-learning as $\tilde{\mathcal{Q}}_t = H_{t, n_t, N_t, L_t, 2U} := \{f \in H_{t, n_t, N_t, L_t} :$

$\|f\|_{L^\infty} \leq 2U$. Then, Q-functions can be defined by $\hat{Q}_{T,n_{T+1},N_{T+1},N_{T+1},L_{T+1}} = 0$ and for $1 \leq t \leq T$,

$$\hat{Q}_{t,n_t,N_t,L_t}(\mathbf{s}_t, \mathbf{a}_t) = \arg \min_{Q_t \in \mathcal{H}_{t,n_t,N_t,L_t,2U}} \mathbb{E}_n \left[\left(R_t + \max_{a_{t+1}} \hat{Q}_{t+1}(\mathbf{S}_{t+1}, \mathbf{A}_t, a_{t+1}) - Q_t(\mathbf{S}_t, \mathbf{A}_t) \right)^2 \right].$$

The policy derived from Q-learning is defined by

$$\hat{\pi}_{n,N,L} = \{\hat{\pi}_{1,n_1,N_1,L_1}, \dots, \hat{\pi}_{T,n_T,N_T,L_T}\}, \quad (26)$$

where

$$\hat{\pi}_{t,n_t,N_t,L_t}(\mathbf{s}_t, \mathbf{a}_{t-1}) = \arg \max_{a_t \in \hat{\mathcal{A}}_t} \hat{Q}_{t,n_t,N_t,L_t}(\mathbf{s}_t, \mathbf{a}_{t-1}, a_t), \quad t = 1, \dots, T. \quad (27)$$

5.2 Power of depth in deep Q-learning

In this subsection, we derive the generalization error for deep Q-learning under the aforementioned assumptions. Our first result shows the power of depth in deep Q-learning when optimal Q-functions are spatially sparse and piecewise constant.

Theorem 4: Under Assumptions 1, 2, 4, 5, and 6, if $\hat{\pi}_{N,\tau}$ is defined by (24) with $\tau = \mathcal{O}(N^{\tilde{d}_t-1} s^{-1} m^{-1})$, then

$$E[V^*(S_1) - V_{\hat{\pi}_{N,\tau}}(S_1)] \leq \hat{C}_1 \mathcal{J}_{p,T} \left(\frac{\log m}{m} \right)^{1/2} \cdot \sum_{t=1}^T \sum_{j=t}^T (3\mu)^{j-t} N_t^{\max\{\tilde{d}_j, \tilde{d}_{j+1}\}/2} (\log N_j)^{1/2}, \quad (28)$$

where \hat{C}_1 is a constant depending only on r, p , and U .

The use of deep nets to learn discontinuous functions in the framework of supervised learning was first studied in [61]. In Theorem 4, we extend their result from supervised learning to RL by using the oracle inequality in Theorem 1. Noting that shallow nets [23] and linear models [60] have difficulties in realizing either the spatial sparseness or piecewise-constant property of optimal Q-functions, the corresponding generalization error is worse than the established results in Theorem 4. As a consequence, traditional Q-learning requires many more samples than deep Q-learning to finish a specific learning task. This demonstrates the power of depth and explains why deep Q-learning performs so well in numerous applications. The following corollary shows the generalization error of deep Q-learning when the Markov assumption is imposed.

Corollary 2: Under Assumptions 1-6, if $d_{a,1} = \dots = d_{a,T} = d_a$, $d_{s,t} = \dots = d_{s,T} = d_s$, $N_1 = \dots = N_T = N$, and $\hat{\pi}_{N,\tau}$ is defined by (24) with $\tau = \mathcal{O}(N^{(d_a+d_s)-1} s^{-1} m^{-1})$, then

$$E[V^*(S_1) - V_{\hat{\pi}_{N,\tau}}(S_1)] \leq \hat{C}_1 \mathcal{J}_{p,T} \left(\frac{N^{d_a+d_s} \log N \log m}{m} \right)^{1/2} \cdot \left(\frac{T}{1-3\mu} - \frac{3\mu(1-(3\mu)^T)}{1-3\mu} \right) \quad (29)$$

Our next theorem shows the generalization error of deep Q-learning in learning spatially sparse and smooth optimal Q-functions.

Theorem 5: Under Assumptions 1, 2, 4, 5 and 7, if $\hat{\pi}_{n,N,L}$ is defined by (26) with

$$n_t = \left(\frac{m s_t^2}{N_t^{\max\{\tilde{d}_{t+1}, \tilde{d}_t\} + 2\tilde{d}_t/p}} \right)^{\frac{\tilde{d}_t}{2r+\tilde{d}_t}}, \quad t = 1, \dots, T,$$

then

$$E[V^*(S_1) - V_{\hat{\pi}_{n,N,L}}(S_1)] \leq \hat{C}_2 \mathcal{J}_{p,T} \sum_{t=1}^T \sum_{j=t}^T (3\mu)^{j-t} m^{-\frac{r}{2r+\tilde{d}_j}} s_j^{\frac{\tilde{d}_j}{2r+\tilde{d}_j}} \cdot N_j^{\frac{pr \max\{\tilde{d}_{j+1}, \tilde{d}_j\} - \tilde{d}_j^2}{(2r+\tilde{d}_j)p}} (\max\{\tilde{d}_j, \tilde{d}_{j+1}\})^{\frac{3}{2}} \log(mN_j),$$

where \hat{C}_2 is a constant depending only on r, p , and U .

Since we consider a general case for deep Q-learning, the generalization error established in Theorem 5 seems a little bit overly sophisticated, by showing its dependence on the smoothness r_t , sparsity s_t , number of partitions N_t , dimension \tilde{d}_t , distortion $\mathcal{J}_{p,T}$, probability parameter μ , and size of samples m . We shall discuss the impact of each factor and simplify our result in the rest of this section. As shown in Theorem 3, obtaining an approximation accuracy of order $\mathcal{O}(n^{-r/d_s} N^{-d/p})$ requires a number of free parameters equal to at least $\mathcal{O}(nN^d)$. This shows a bias-variance trade-off by noting that the capacity of deep nets depends heavily on the number of free parameters. Under these conditions, n_t in Theorem 4 is selected to balance the bias and variance. Since the reward functions in Q-learning are practically extremely sparse, the sparsity s_t , compared with the number of partitions $N_t^{\tilde{d}_t}$, is often extremely small, which together with $pr \leq \min_{1 \leq j \leq T} \tilde{d}_j$ yields very good generalization error estimates for deep Q-learning. In the following, we present a corollary for Theorem 5 under added assumptions to explicitly exhibit the generalization error.

Corollary 3: Under Assumptions 1-5 with $p = 2$ and Assumption 7, if $d_{a,1} = \dots = d_{a,T} = d_a$, $d_{s,t} = \dots = d_{s,T} = d_s$, $s_1 = \dots = s_T = s$, $r_1 = \dots = r_T = r$, $N_1 = \dots = N_T = N$, and

$$n = \left(\frac{m s^2}{N^{2d_a+2d_s}} \right)^{\frac{d_a+d_s}{2r+d_a+d_s}},$$

then

$$E[V^*(S_1) - V_{\hat{\pi}_{n,N,L}}(S_1)] \leq \hat{C}_3 m^{-\frac{r}{2r+d_a+d_s}} \log(mN) s^{\frac{d_a+d_s}{2r+d_a+d_s}} \cdot N^{\frac{(2r-d_a-d_s)(d_a+d_s)}{4r+2d_a+2d_s}} \sum_{t=1}^T \left(\frac{T}{1-3\mu} - \frac{3\mu(1-(3\mu)^T)}{1-3\mu} \right),$$

where \hat{C}_3 is a constant independent of N, s, m , or T .

From Corollary 3, a generalization error bound of order $\mathcal{O}(m^{-\frac{r}{2r+d_a+d_s}} N^{\frac{(2r-d_a-d_s)(d_a+d_s)}{4r+2d_a+2d_s}} s^{\frac{d_a+d_s}{2r+d_a+d_s}})$ is derived. If r is large, then the dominant term is $m^{-\frac{r}{2r+d_a+d_s}}$. Under this circumstance, numerous data are required to produce a high-quality policy, just as AlphaGo did in [5]. If r

is relatively small, then $N^{\frac{(2r-d_a-d_s)(d_a+d_s)}{4r+2d_a+2d_s}} \frac{d_a+d_s}{s^{2r+d_a+d_s}}$ is the dominant term, implying that there are a few candidates available to make a decision, which is also popular in practice [3]. Furthermore, given that the linear models and shallow nets cannot approximate the spatially sparse and piecewise smooth functions well [23], [42], it is difficult to derive a similar result for traditional Q-learning as Theorem 4 and Corollary 3, which demonstrates the power of depth in deep Q-learning.

To end this section, we differentiate our results are from those of [43], where theoretical verification is also conducted for deep Q-learning. As discussed in Sec. 1.3, the setting in [43] is available for RL with infinite horizons and requires strong assumptions on the optimal Q-functions and likelihood P (defined by (1)), which are difficult to check in practice. As shown in Sec. 3.1, Assumptions 2, 5, 6, and 7 on Q_t^* are easily satisfied for numerous real-world applications (e.g., Table 4.1). Furthermore, we only impose two extra assumptions including Assumptions 1 and 5 on the likelihood P , which is essentially looser than the concentration coefficient assumption in [43] and easily satisfied in practice. The weakness of the assumptions and availability in practice are main the reasons that our derived generalization error bounds behave exponentially badly in the time horizon. It would be interesting to find more suitable assumptions from real-world applications to reduce this negative effect.

6 EXPERIMENTAL RESULTS

In this section, we apply deep Q-learning to the beer game, a well-known supply chain management problem, and a recommender system application, to illustrate the roles of the depth of neural networks, rewards, and data size in RL.

6.1 Beer Game Experiment

The first experiment is conducted in the context of an inventory management problem, named the Beer Game. Beer Game is a multi-agent supply chain management problem, with four agents participating, from upstream to downstream of which are the manufacturer, distributor, warehouse and retailer. In each period of the game, each agent observes the current inventory state and decides on an order to send to his predecessor (supplier). We examine how DQN can help agents decide on the right orders to minimize the total inventory in hand over a long time. The detailed introduction as well as an RL framework of the beer game can be found in Section 4 of the supplementary material. We report our experiment designs and numerical results in the following subsections. Each subsection contains experiments based on simulations and three real-world data sets. The experimental settings based on the simulated data and real-world data sets are given in Section 5 and Section 6 of the supplementary material.

6.1.1 Power of the depth

Our first simulation focuses on the power of depth in deep Q-learning. According to Theorems 4 and 5, the effect of depth depends heavily on the reward property. Therefore, we use the shaped reward in [14] in this simulation and record our method as shaped reward deep Q-networks

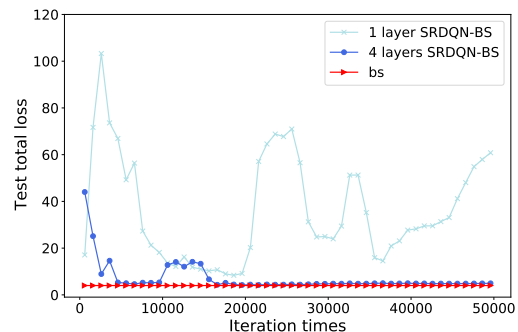


Fig. 6. Performance of SRDQN-BS policy with different-depth-SRDQN

(SRDQN). The based stock policy (bs for short) is regarded as a baseline. As there are four agents in the beer game, we only apply deep Q-learning on the first agent while applying bs on the three remaining agents. In this way, we record our approach as shaped reward deep Q-networks and based stock policy (SRDQN-BS). For further clarity, we refer the readers to Section 4 and Section 5 of the supplementary material for details.

As shown in Section 4 of the supplementary material, the reward, as a function of actions, possesses the spatially sparse and piecewise constancy property. Our theoretical assertions suggest that deep learning outperforms the classical (shallow) approach in such an RL problem. To verify this, we test the SRDQN-BS policy with five cases, with one, two, three, four, and five hidden layers in the SRDQN. Results of the one- and four-layer cases are shown in Figure 6.

From Figure 6, there are three interesting observations: (1) The test total loss of the four-layers SRDQN-BS is much less than that of the one-layer SRDQN-BS, showing that deepening the network is crucial for improving the performance of the classical shallow learning policy. (2) After a few iterations, the prediction of four-layer SRDQN-BS stabilizes, showing that it can generalize well, which is beyond the capability of the one-layer SRDQN-BS. This verifies Theorem 4 in the sense that the variance of deep Q-learning is not large, since deepening the network does not essentially enlarge the capacity of hypothesis space. (3) After 15000 iterations, four-layer SRDQN-BS performs almost as well as bs, showing that our adopted approach can achieve an almost optimal generalization performance. All these observations show that depth plays an important role in deep Q-learning if spatially sparse and piecewise constant rewards are utilized.

To show the power of depth and stability of SRDQN-BS with different layers, we also extract the best-performance-segment of SRDQN-BS with consecutive iterations 5000, 10000 and 20000 of five cases, as compared in Figure 7.

Two interesting phenomena are exhibited in Figure 7: (1) Before a threshold value ($L=4$ in this simulation), depth plays a positive role in SRDQN-BS. This shows again the power of depth in deep Q-learning. (2) After the threshold value, depth is not so important in generalization, since five-layer SRDQN-BS performs a little bit worse than the four-layer policy. This does not contradict our theoretical assertions. In fact, according to our proofs in the supplementary

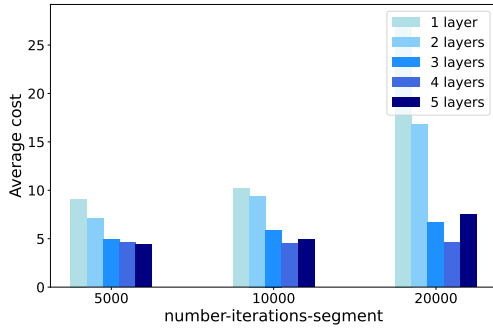


Fig. 7. Best-performance-segment of SRDQN-BS policy with different iteration ranges

material, the constants \hat{C}_1 and \hat{C}_2 depend on the number of layers, which may cause a small oscillation. Furthermore, the covering number estimate (Lemma 1) shows that the capacity of deep nets increases as they are deepened, leading to an instability phenomenon for five-layer SRDQN-BS.

We further conduct experiments based on real-world historical demand data for three different items to examine the power of depth in deep Q-learning. The training process of one- and three-layer SRDQN-BS policy is shown in Figure 8, where the bs policy acts as the optimal baseline.

The findings are quite similar to those in synthetic simulations. It’s clear that depth is essential for good performance of SRDQN. In all three experiments, SRDQN with 3 layers converges to a stable point with a small total loss more quickly than SRDQN with 1 layer. In the experiment of item 34, SRDQN with 1 layer even doesn’t converge in the end. The second point that deserves to be noticed is that the convergence point of SRDQN-BS policy with 3 layers is pretty close to bs policy in all three experiments, which indicates that it achieves near-optimal performance. This shows the strong generalization ability of the SRDQN-BS policy with 3 layers.

We conduct a more comprehensive comparison by extracting the performance of SRDQN-BS at different training iterations. We implement SRDQN-BS with 1 layer, 3 layers, 5 layers, and 7 layers. The results are shown in Figure 9.

Clearly, the SRDQN-BS policy with 1 layer performs badly while the SRDQN-BS policy with 3 layers performs quite well. However, continuing to increase the depths in SRDQN, such as increasing to 5 and 7 layers, doesn’t keep improving performance but worsens the performance. This is because deeper nets lead to instability in the training process.

6.1.2 Influence of different rewards

In this simulation, we shall show the important role of reward in deep Q-learning. We use the classical rewards in the beer game (see Section 4 of the supplementary material) rather than the shaped one proposed in [14] and then obtain the deep Q-learningbs (DQNBS) policy. DQN-BS and SRDQN-BS differ only in their rewards. Comparison of DQN-BS and SRDQN-BS policy with one-layer and four-layers are shown in Figure 10.

Figure 10 exhibits three important findings: (1) From Figure 10 (a), if the hypothesis space is not appropriately selected, then rewards do not affect the performance of Q-learning substantially. This shows the necessity of taking different hypothesis spaces in Q-learning and implies the importance of Theorem 1. (2) From Figure 10 (b), when the suitable hypothesis space is used, then rewards are key to improving the performance of Q-learning. The perfect performance of SRDQN-BS is based on suitable rewards and hypothesis space, which verifies Theorems 2 and 3; (3) As shown in Section 4 of the supplementary material, the rewards of DQN-BS are also spatially sparse and piecewise constant. As compared with the rewards of SRDQN-BS, the only difference is that there are many more pieces in DQN-BS. According to Theorems 4 and 5, the generalization error of DQN-BS should be worse than that of SRDQN-BS. This assertion is verified by comparing Figures 10 (a) and 10 (b). In particular, deep Q-learning improves the performance of shallow Q-learning significantly for SRDQN-BS, while conservatively for DQN-BS.

We report the comparison of SRDQN-BS policy and DQN-BS policy on three real-world datasets in Figure 11. We can see that even with 3 layers, the DQN-BS policy can hardly converge, and it performs much worse than the SRDQN-BS policy with 3 layers. This indicates that reward with nice properties is crucial for the power of deep Q-learning.

6.1.3 Influence of data size

In our last simulation, we devoted ourselves to studying the role of data size in deep Q-learning by investigating how the performance of SRDQN changes with respect to data size. Unlike in the above experiments that draw the sample with replacement, we draw the sample without replacement to show the role of data size. Specifically, we sample 16 examples from replay memory and discard them after training. By doing this, we relate the number of iterations with the number of samples. After 500 iterations, meeting the minimum experience replay size to start training, 100 samples are used to train SRDQN per iteration. We test the SRDQN-BS policy with two cases (one and four hidden layers of neural networks). The simulation results are shown in Figure 13.

Based on Figure 13, we can draw the following three conclusions: (1) As shown in Theorem 1, the required size of the sample to guarantee the generalization performance of Q-learning behaves exponentially with T , which implies that SRDQN-BS needs large samples. This demonstrates the poor performance of SRDQN-BS when the data size is smaller than 1,500,000. (2) According to Theorem 4, compared with shallow Q-learning, deep Q-learning requires fewer samples to achieve the same long-term rewards. Therefore, the increasing number of samples gradually offsets the negative effects of long-term Q-learning. As a result, the test total cost begins to decrease with respect to the number of samples, as the data size interval changes from 1,500,000 to 3,500,000. However, shallow Q-learning still oscillates because it requires much more samples. (3) After the training of 3,500,000 samples, the four-layer SRDQN-BS converges to a stable state and performs almost the same as the bs, showing that this policy can achieve the

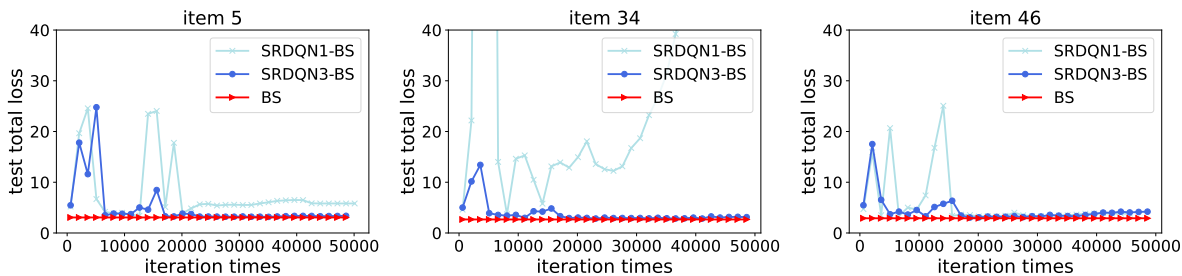


Fig. 8. Performance of SRDQN-BS policy with different-depth-SRDQN

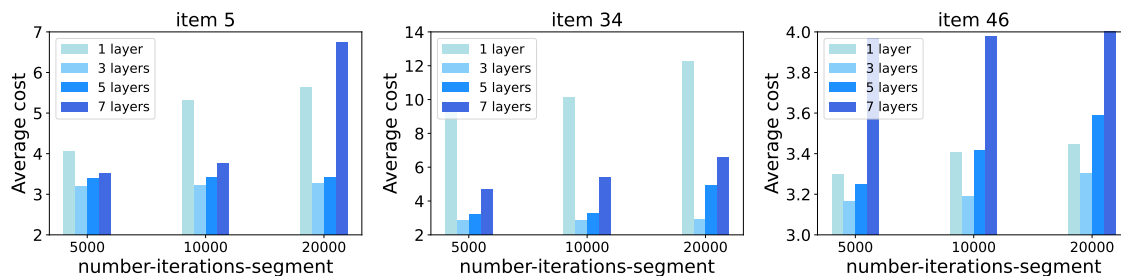


Fig. 9. Best-performance-segment of SRDQN-BS policy with different iteration ranges

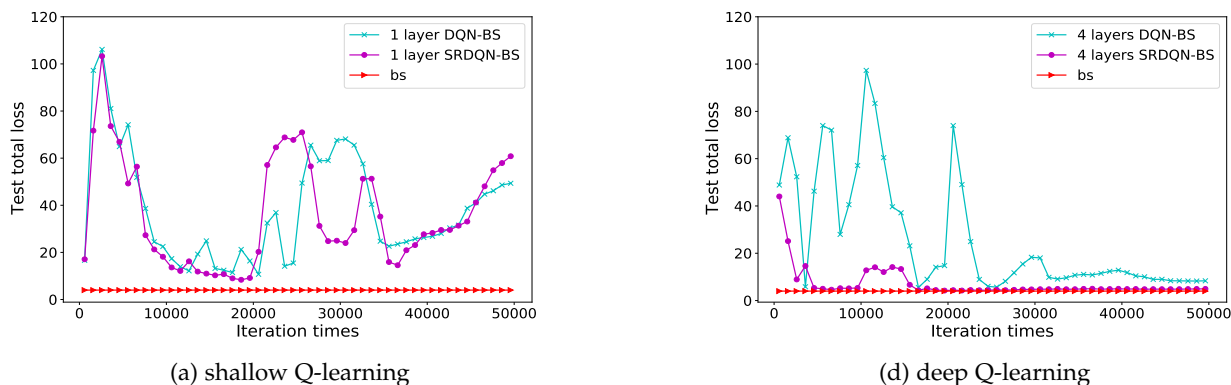


Fig. 10. Comparison of DQN-BS policy and SRDQN-BS policy with different depth

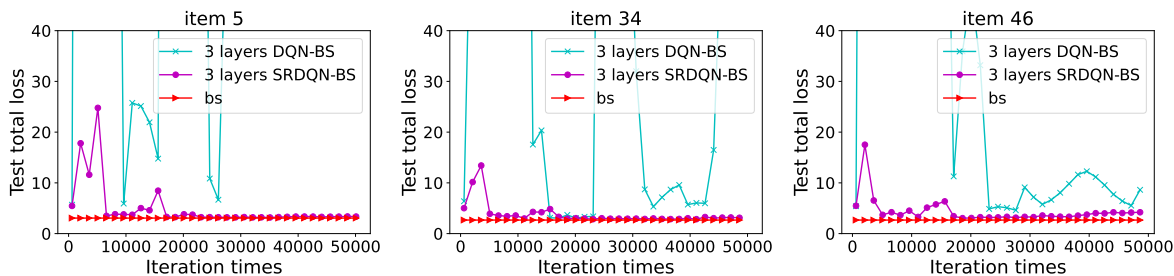


Fig. 11. Comparison of DQN-BS policy and SRDQN-BS policy with different depth

optimal generalization performance, and 3,500,000 is almost the smallest data size needed to guarantee the optimal generalization performance of deep Q-learning in this beer game.

We test the SRDQN-BS policy with 1 layer and 3 layers on three real-world datasets. The results are shown in Figure 12. The result shows that the SRDQN-BS policy with

3 layers converges to near-optimal after approximately 3 million samples. However, shallow nets diverge after certain periods of training, and it can never achieve near-optimal performance.

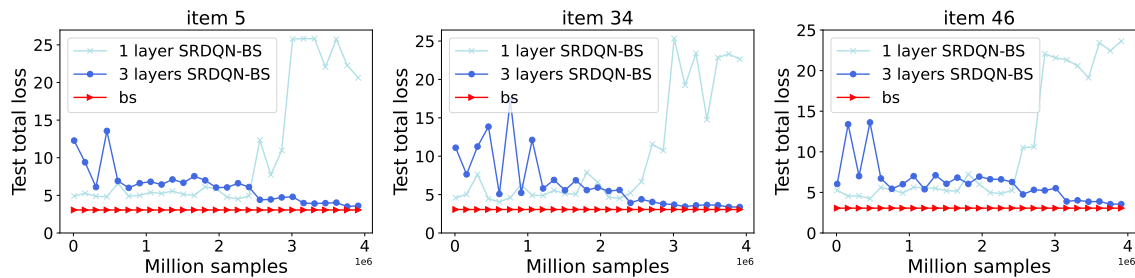


Fig. 12. Role of data size in SRDQN-BS

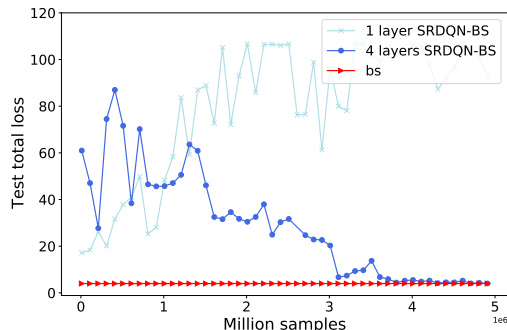


Fig. 13. Role of data size in SRDQN-BS

6.2 Recommender System Experiment

We conduct a second experiment in the context of the recommender system. We look forward to providing criteria for choosing and designing Q-learning frameworks in recommender systems by answering the three questions that we are interested in. Different RL algorithms have been applied to designing recommender systems [24], [62], due to the long-term reward maximization nature of reinforcement learning. We conduct experiments on a simulation recommender system platform called Recsim [44]. In this simulated recommender system, we use DQN to recommend a set of items for a certain user at each period over a long time. We aim to maximize long-term user engagement, considering user interest shifts. We examine DQN with different depths, with expected reward, which possesses the spatially sparse and piecewise constancy property, and standard reward. The detailed recommender system context that we consider and the RL framework is introduced in Section 7 of the supplementary material. In the following, we describe how to conduct experiments to investigate the aforementioned three different points and how the experimental results verify our theoretical results.

Firstly, we check the power of depth in DQN with the standard reward (DQN-s). The result is shown in Figure 14. Clearly, DQN-s with 1 layer perform worst. Although DQN-s with 3 layers, 5 layers, and 8 layers are better than DQN-s with 1 layer, they can't achieve an obvious improvement in the training process. This indicates that DQNs can't learn a proper recommendation policy even with a deep net.

Next, we replace the standard reward with the expected reward, leading to the DQN with the expected reward (DQN-e). The result is shown in Figure 15. We can see that

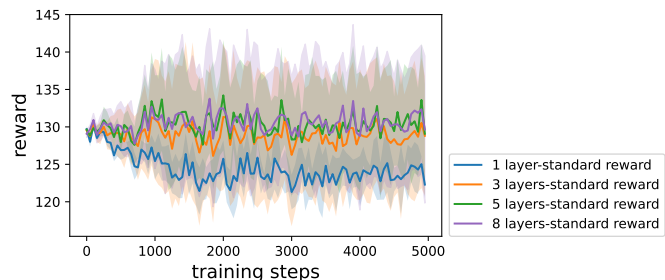


Fig. 14. Performance of DQN with different depths and standard reward

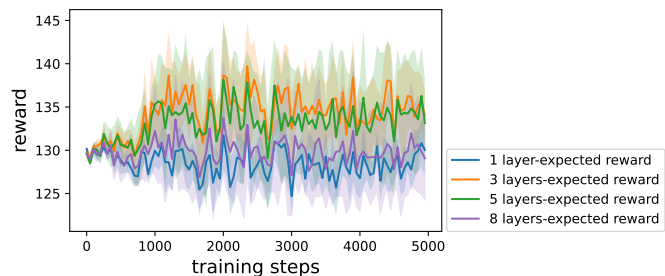


Fig. 15. Performance of DQN with different depths and expected reward

DQN-e with 1 layer still performs badly. But when the net becomes deeper, i.e., DQN-e with 3 layers and 5 layers, the performance improves obviously after around 1000 training steps. This shows that DQN-e with a proper deep net can perform well in this recommendation task, and so the power of depth in DQN has been shown. On the other hand, when it comes to DQN-e with 8 layers, the performance decreases. This reveals the trade-off between capacity and stability of the deep nets.

In order to show the effectiveness of the learned policy, we compare DQN-e with 3 layers with two benchmarks. The first benchmark is the Random policy, which randomly samples two documents for recommendation each time t . The second benchmark is called Myopic, which means that we train a net without considering long-term reward maximization. Specifically, when we train the DQN net, we

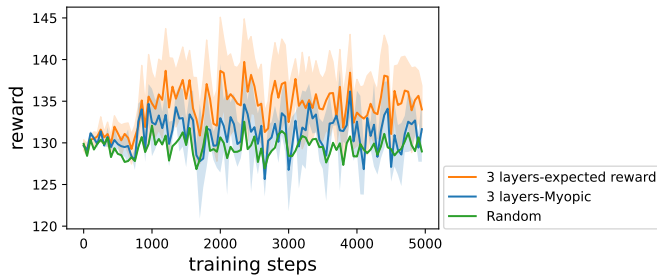


Fig. 16. Comparison of benchmarks and DQN with expected reward

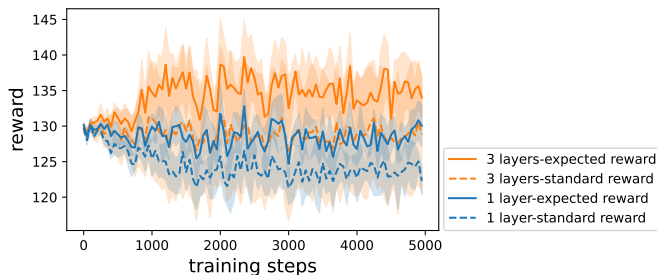


Fig. 17. comparison between DQN with standard reward and DQN with expected reward

update the net in the following form:

$$Q^{(t)}(s, A) \leftarrow \alpha^{(t)} \left[r + \max_{A'} \gamma Q^{(t-1)}(s', A') \right] + (1 - \alpha^{(t)}) Q^{(t-1)}(s, A)$$

In Myopic, we set γ as 0 to optimize only the immediate reward. We set the net in Myopic policy as the same net in DQN-e. The result is shown in Figure 16. We can see that the mean reward of the Random policy is approximately a horizontal line. The Myopic policy is better than the Random policy but worse than DQN-e, which shows the importance of considering state transitions and long-term reward maximization.

We compare the performance of DQN-s and DQN-e with different layers in Figure 17. We can reveal the power of DQN only with both proper reward function and proper depth. The management implications here are that DQN is not almighty without any precondition. The first thing we must decide is a reward function with the nice property we proposed in our theory. The second is to decide on a proper depth to uncover the full ability of the DQN method.

Finally, we examine the role of sample size in DQN-e. Here we discard the used samples in the way described in the Beer Game experiment. We try DQN-e with 1 layer, 3 layers, and 8 layers. The results are reported in Figure 18. It's clear that the performance of DQN-e with 3 layers improves to a stable point after the first 3000 samples, while DQN-e with 1 layer and 8 layers can't converge even after more than 10000 samples.

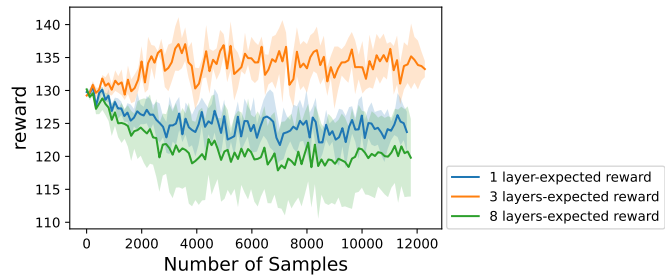


Fig. 18. Role of data size in DQN with expected reward

7 CONCLUSION

In this paper, we demonstrate the power of depth in deep Q-learning by showing its better generalization error bounds compared with those of the traditional version. Our main tools are a novel oracle inequality for Q-learning to show the importance of hypothesis spaces, two novel approximation theorems to show the expressive power of deep nets, and two generalization error estimates to exhibit the power of depth in deep Q-learning. We find that the main reason for the success of deep Q-learning is the outperformance of deep nets in approximating spatially sparse and piecewise smooth (or piecewise constant) functions, rather than its large capacity. Our study has provided answers to Questions 1-3 in Sec. 1.1.

◊ **Answer to Question 1.** As shown in Section 3.1, the most widely used reward functions in Q-learning are spatially sparse and piecewise constant (or piecewise smooth). Deep nets succeed in capturing these properties (see Theorems 2 and 3), which is beyond the capability of shallow nets or linear models [23], [42]. Thus, deep Q-learning performs much better than shallow nets and linear models in practice.

◊ **Answer to Question 2.** As discussed in Sec. 3.2, deep Q-learning does not always outperform the traditional Q-learning. However, if reward functions in Q-learning possess certain sophisticated properties such as spatial sparseness, piecewise smoothness, piecewise constancy, and the properties in Table 2, then deep Q-learning performs better than shallow nets.

◊ **Answer to Question 3.** The required sample size to finish a specific sequential decision-making problem depends on the properties of reward functions and the horizon T . Our results in Theorem 4, Theorem 5, Corollary 2, and Corollary 3 quantified this relationship in terms of generalization error bounds.

REFERENCES

- [1] L. Schultz and V. Sokolov, "Deep reinforcement learning for dynamic urban transportation problems," *arXiv preprint arXiv:1806.05310*, 2018.
- [2] I. Giannoccaro and P. Pontrandolfo, "Inventory management in supply chains: a reinforcement learning approach," *International Journal of Production Economics*, vol. 78, no. 2, pp. 153–161, 2002.
- [3] G. Zheng, F. Zhang, Z. Zheng, Y. Xiang, N. J. Yuan, X. Xie, and Z. Li, "Dqn: A deep reinforcement learning framework for news recommendation," in *Proceedings of the 2018 World Wide Web Conference*, 2018, pp. 167–176.
- [4] G. Gallego and G. Van Ryzin, "Optimal dynamic pricing of inventories with stochastic demand over finite horizons," *Management Science*, vol. 40, no. 8, pp. 999–1020, 1994.

- [5] D. Silver, A. Huang, C. J. Maddison, A. Guez, L. Sifre, G. Van Den Driessche, J. Schrittwieser, I. Antonoglou, V. Panneershelvam, M. Lanctot *et al.*, "Mastering the game of go with deep neural networks and tree search," *Nature*, vol. 529, no. 7587, p. 484, 2016.
- [6] D. Kalashnikov, A. Irpan, P. Pastor, J. Ibarz, A. Herzog, E. Jang, D. Quillen, E. Holly, M. Kalakrishnan, V. Vanhoucke *et al.*, "Qt-opt: Scalable deep reinforcement learning for vision-based robotic manipulation," *arXiv preprint arXiv:1806.10293*, 2018.
- [7] W. L. Winston and J. B. Goldberg, *Operations Research: Applications and Algorithms*. Thomson Brooks/Cole Belmont, 2004, vol. 3.
- [8] A. Mascis and D. Pacciarelli, "Job-shop scheduling with blocking and no-wait constraints," *European Journal of Operational Research*, vol. 143, no. 3, pp. 498–517, 2002.
- [9] P. Rusmevichientong, B. Van Roy, and P. W. Glynn, "A nonparametric approach to multiproduct pricing," *Operations Research*, vol. 54, no. 1, pp. 82–98, 2006.
- [10] Z.-H. Zhou, N. V. Chawla, Y. Jin, and G. J. Williams, "Big data opportunities and challenges: Discussions from data analytics perspectives [discussion forum]," *IEEE Computational Intelligence Magazine*, vol. 9, no. 4, pp. 62–74, 2014.
- [11] D. Russo and B. Van Roy, "Learning to optimize via information-directed sampling," *Operations Research*, vol. 66, no. 1, pp. 230–252, 2018.
- [12] M. Kraus, S. Feuerriegel, and A. Oztekin, "Deep learning in business analytics and operations research: Models, applications and managerial implications," *European Journal of Operational Research*, vol. 281, no. 3, pp. 628–641, 2020.
- [13] H. Yoganarasimhan, "Search personalization using machine learning," *Management Science*, vol. 66, no. 3, pp. 1045–1070, 2020.
- [14] A. Oroojlooyjadid, M. Nazari, L. V. Snyder, and M. Takáč, "A deep q-network for the beer game: Deep reinforcement learning for inventory optimization," *Manufacturing & Service Operations Management*, vol. 24, no. 1, pp. 285–304, 2022.
- [15] Y. Bengio, A. Courville, and P. Vincent, "Representation learning: A review and new perspectives," *IEEE Transactions on Pattern Analysis and Machine Intelligence*, vol. 35, no. 8, pp. 1798–1828, 2013.
- [16] R. S. Sutton and A. G. Barto, *Reinforcement Learning: An Introduction*. MIT press, 2018.
- [17] I. Popescu and Y. Wu, "Dynamic pricing strategies with reference effects," *Operations Research*, vol. 55, no. 3, pp. 413–429, 2007.
- [18] A. Gosavi, "Reinforcement learning: A tutorial survey and recent advances," *INFORMS Journal on Computing*, vol. 21, no. 2, pp. 178–192, 2009.
- [19] C. J. Watkins and P. Dayan, "Q-learning," *Machine Learning*, vol. 8, no. 3–4, pp. 279–292, 1992.
- [20] M. Sugiyama, *Statistical Reinforcement Learning: Modern Machine Learning Approaches*. CRC Press, 2015.
- [21] J. Peters and S. Schaal, "Reinforcement learning of motor skills with policy gradients," *Neural Networks*, vol. 21, no. 4, pp. 682–697, 2008.
- [22] F. Cucker and D. X. Zhou, *Learning Theory: An Approximation Theory Viewpoint*. Cambridge University Press, 2007, vol. 24.
- [23] C. Chui, X. Li, and H. N. Mhaskar, "Neural networks for localized approximation," *Mathematics of Computation*, vol. 63, no. 208, pp. 607–623, 1994.
- [24] E. Ie, V. Jain, J. Wang, S. Narvekar, R. Agarwal, R. Wu, H.-T. Cheng, M. Lustman, V. Gatto, P. Covington *et al.*, "Reinforcement learning for slate-based recommender systems: A tractable decomposition and practical methodology," *arXiv preprint arXiv:1905.12767*, 2019.
- [25] V. François-Lavet, P. Henderson, R. Islam, M. G. Bellemare, J. Pineau *et al.*, "An introduction to deep reinforcement learning," *Foundations and Trends in Machine Learning*, vol. 11, no. 3–4, pp. 219–354, 2018.
- [26] J. Tsitsiklis and B. Vanroy, "An analysis of temporal-difference learning with function approximation," *IEEE Transactions on Automatic Control*, vol. 42, no. 5, pp. 674–690, 1997.
- [27] E. Even-Dar and Y. Mansour, "Learning rates for q-learning," *Journal of Machine Learning Research*, vol. 5, no. Dec, pp. 1–25, 2003.
- [28] H. Yu and D. P. Bertsekas, "Convergence results for some temporal difference methods based on least squares," *IEEE Transactions on Automatic Control*, vol. 54, no. 7, pp. 1515–1531, 2009.
- [29] S. A. Murphy, "A generalization error for q-learning," *Journal of Machine Learning Research*, vol. 6, pp. 1073–1097, 2005.
- [30] M. J. Kearns and S. P. Singh, "Finite-sample convergence rates for q-learning and indirect algorithms," in *Advances in Neural Information Processing Systems*, 1999, pp. 996–1002.
- [31] Y. Goldberg and M. R. Kosorok, "Q-learning with censored data," *Annals of Statistics*, vol. 40, no. 1, pp. 529–560, 2012.
- [32] G. Dalal, B. Szörényi, G. Thoppe, and S. Mannor, "Finite sample analyses for td (0) with function approximation," in *Proceedings of Thirty-Second AAAI Conference on Artificial Intelligence*, 2018, pp. 6144–6153.
- [33] S. Zou, T. Xu, and Y. Liang, "Finite-sample analysis for sarsa with linear function approximation," in *Advances in Neural Information Processing Systems*, 2019, pp. 8665–8675.
- [34] M. J. Wainwright, "Variance-reduced q-learning is minimax optimal," *arXiv preprint arXiv:1906.04697*, 2019.
- [35] G. Cybenko, "Approximation by superpositions of a sigmoidal function," *Mathematics of Control, Signals and Systems*, vol. 2, no. 4, pp. 303–314, 1989.
- [36] Z.-C. Guo, L. Shi, and S.-B. Lin, "Realizing data features by deep nets," *IEEE Transactions on Neural Networks and Learning Systems*, vol. 31, no. 10, pp. 4036–4048, 2020.
- [37] U. Shaham, A. Cloninger, and R. R. Coifman, "Provable approximation properties for deep neural networks," *Applied and Computational Harmonic Analysis*, vol. 44, no. 3, pp. 537–557, 2018.
- [38] C. Schwab and J. Zech, "Deep learning in high dimension: Neural network expression rates for generalized polynomial chaos expansions in uq," *Analysis and Applications*, vol. 17, no. 1, pp. 19–55, 2019.
- [39] S.-B. Lin, "Generalization and expressivity for deep nets," *IEEE Transactions on Neural Networks and Learning Systems*, vol. 30, no. 5, pp. 1392–1406, 2018.
- [40] C. K. Chui, S.-B. Lin, and D.-X. Zhou, "Deep neural networks for rotation-invariance approximation and learning," *Analysis and Applications*, vol. 17, no. 05, pp. 737–772, 2019.
- [41] H. N. Mhaskar and T. Poggio, "Deep vs. shallow networks: An approximation theory perspective," *Analysis and Applications*, vol. 14, no. 06, pp. 829–848, 2016.
- [42] P. Petersen and F. Voigtlaender, "Optimal approximation of piecewise smooth functions using deep relu neural networks," *Neural Networks*, vol. 108, pp. 296–330, 2018.
- [43] J. Fan, Z. Yang, Y. Xie, and Z. Wang, "A theoretical analysis of deep q-learning," *arXiv preprint arXiv:1901.00137v3*, 2020.
- [44] E. Ie, C.-w. Hsu, M. Mladenov, V. Jain, S. Narvekar, J. Wang, R. Wu, and C. Boutilier, "Recsim: A configurable simulation platform for recommender systems," *arXiv preprint arXiv:1909.04847*, 2019.
- [45] R. Bellman, "Dynamic programming," *Science*, vol. 153, no. 3731, pp. 34–37, 1966.
- [46] S. M. Kakade, "On the sample complexity of reinforcement learning," Ph.D. dissertation, University of London, London, England, 2003.
- [47] L. Györfi, M. Kohler, A. Krzyzak, and H. Walk, *A Distribution-Free Theory of Nonparametric Regression*. Springer Science & Business Media, 2006.
- [48] I. Steinwart and A. Christmann, *Support Vector Machines*. Springer Science & Business Media, 2008.
- [49] S.-B. Lin and D.-X. Zhou, "Distributed kernel-based gradient descent algorithms," *Constructive Approximation*, vol. 47, no. 2, pp. 249–276, 2018.
- [50] G. Shani, D. Heckerman, and R. I. Brafman, "An mdp-based recommender system," *Journal of Machine Learning Research*, vol. 6, no. Sep, pp. 1265–1295, 2005.
- [51] D.-X. Zhou, "Theory of deep convolutional neural networks: Downsampling," *Neural Networks*, vol. 124, pp. 319–327, 2020.
- [52] D.-X. Zhou, "Universality of deep convolutional neural networks," *Applied and Computational Harmonic Analysis*, vol. 48, no. 2, pp. 787–794, 2020.
- [53] M. Anthony and P. L. Bartlett, *Neural Network Learning: Theoretical Foundations*. Cambridge University Press, 2009.
- [54] H. N. Mhaskar, "Neural networks for optimal approximation of smooth and analytic functions," *Neural Computation*, vol. 8, no. 1, pp. 164–177, 1996.
- [55] D. Yarotsky, "Error bounds for approximations with deep relu networks," *Neural Networks*, vol. 94, pp. 103–114, 2017.
- [56] S.-B. Lin, "Limitations of shallow nets approximation," *Neural Networks*, vol. 94, pp. 96–102, 2017.
- [57] C. K. Chui, S.-B. Lin, B. Zhang, and D.-X. Zhou, "Realization of spatial sparseness by deep relu nets with massive data," *IEEE Transactions on Neural Networks and Learning Systems*, vol. 33, no. 1, pp. 229–243, 2020.
- [58] Z. Han, S. Yu, S.-B. Lin, and D.-X. Zhou, "Depth selection for deep relu nets in feature extraction and generalization," *IEEE*

Transactions on Pattern Analysis and Machine Intelligence, vol. 44, no. 4, pp. 1853–1868, 2022.

- [59] A. Pinkus, “Approximation theory of the mlp model in neural networks,” *Acta Numerica*, vol. 8, pp. 143–195, 1999.
- [60] B. Llanas, S. Lantarón, and F. J. Sáinz, “Constructive approximation of discontinuous functions by neural networks,” *Neural Processing Letters*, vol. 27, no. 3, pp. 209–226, 2008.
- [61] M. Imaizumi and K. Fukumizu, “Deep neural networks learn non-smooth functions effectively,” *arXiv preprint arXiv:1802.04474*, 2018.
- [62] M. M. Afsar, T. Crump, and B. Far, “Reinforcement learning based recommender systems: A survey,” *ACM Computing Surveys*, vol. 55, no. 7, pp. 1–38, 2022.